APPLIED SCIENCES AND ENGINEERING

Strong adhesion of wet conducting polymers on diverse substrates

Akihisa Inoue[1,2]*, Hyunwoo Yuk[1]*, Baoyang Lu[1,3,4], Xuanhe Zhao[1,5]†

Conducting polymers such as poly(3,4-ethylenedioxythiophene):poly(styrene sulfonate) (PEDOT:PSS), polypyrrole (PPy), and polyaniline (PAni) have attracted great attention as promising electrodes that interface with biological organisms. However, weak and unstable adhesion of conducting polymers to substrates and devices in wet physiological environment has greatly limited their utility and reliability. Here, we report a general yet simple method to achieve strong adhesion of various conducting polymers on diverse insulating and conductive substrates in wet physiological environment. The method is based on introducing a hydrophilic polymer adhesive layer with a thickness of a few nanometers, which forms strong adhesion with the substrate and an interpenetrating polymer network with the conducting polymer. The method is compatible with various fabrication approaches for conducting polymers without compromising their electrical or mechanical properties. We further demonstrate adhesion of wet conducting polymers on representative bioelectronic devices with high adhesion strength, conductivity, and mechanical and electrochemical stability.

INTRODUCTION

Conducting polymers such as poly(3,4-ethylenedioxythiophene):poly (styrene sulfonate) (PEDOT:PSS), polypyrrole (PPy), and polyaniline (PAni) have been widely explored as electrodes and coatings for electrodes that interface with biological organisms in bioelectronic devices (*1*–*8*), owing to their favorable electrochemical stability (*9*), electrical and mechanical properties (*10*–*16*), and biocompatibility (*13*, *17*, *18*). However, weak and unstable adhesion of conducting polymers on substrates and devices can result in interfacial failures (e.g., debonding of conducting polymers) and subsequent loss of functionality, substantially hampering the reliability and efficacy of bioelectronic devices (*5*, *6*, *19*–*23*). In light of this challenge, a few methods have been reported to provide enhanced adhesion of conducting polymers in wet environment. For example, topological modification of substrates (e.g., nano- and microscale roughness on gold substrates) (*24*, *25*) and electrodeposition of chemically modified EDOT monomers (e.g., vinyl-, carboxylic-, and amine-modified EDOT) (*23*, *26*, *27*) have been adopted to improve adhesion of wet PEDOT:PSS. However, the previous approaches require specific types of substrates and/or complicated modification of EDOT monomer, and they are limited to electrodeposited PEDOT:PSS on conductive substrates, substantially limiting the applicability of conducting polymers in bioelectronics devices.

Here, we report a general yet simple method to achieve strong adhesion of various wet conducting polymers including PEDOT:PSS, PPy, and PAni on diverse commonly used insulating and conductive substrates including glass, polyimide, polydimethylsiloxane (PDMS), indium tin oxide (ITO), and gold. The method is based on introducing a hydrophilic polymer adhesive layer with a thickness of a few nanometers between the substrate and the conducting polymer. The adhesive layer forms strong adhesion with the substrate and an interpenetrating polymer network with the conducting polymer. To implement the method, we choose hydrophilic polyurethane (PU) to form the nanometer-thick adhesive layer. The adhesive layer can be facilely introduced on a broad range of substrate materials via diverse fabrication approaches including spin coating, spray coating, and dip coating. The resultant interfacial adhesion between wet conducting polymers and various substrates is strong (e.g., lap-shear strength over 120 kPa) and mechanically and electrochemically stable (e.g., no observable interfacial failure after 60 min of ultrasonication and 10,000 charging and discharging cycles). Our method also allows the use of commercially available conducting polymers and hydrophilic PU without the need for complex chemical synthesis or substrate modification, promising ready and broad applicability to bioelectronic devices. Furthermore, the method is compatible with various fabrication approaches for conducting polymers including solvent casting and electrodeposition, without compromising the electrical or mechanical properties of conducting polymers.

RESULTS

Method for strong adhesion of wet conducting polymers on substrates

Instead of modifying a specific conducting polymer or substrate, we propose a general method to achieve strong adhesion of various wet conducting polymers on diverse substrates by using a hydrophilic polymer adhesive layer with a thickness of a few nanometers, as illustrated in Fig. 1A. To avoid effects from substrates' surface roughness, we use substrates with smooth surfaces (i.e., mean roughness below 5 nm) in this study (fig. S1). A substrate is first functionalized with primary amine groups (fig. S2), which can provide an enhanced interfacial adhesion between the substrate and the adhesive layer via covalent bonds and/or electrostatic interactions (*28*). Thereafter, the adhesive layer can be applied to a wide range of substrates by various coating approaches including spin coating, spray coating, and dip coating. Conducting polymers can then be prepared on the substrate with the adhesive layer from conducting polymer

[1]Department of Mechanical Engineering, Massachusetts Institute of Technology, Cambridge, MA 02139, USA. [2]JSR Corporation, Tokyo 1050021, Japan. [3]Flexible Electronics Innovation Institute, Jiangxi Science and Technology Normal University, Nanchang 330013, China. [4]School of Pharmacy, Jiangxi Science and Technology Normal University, Nanchang 330013, China. [5]Department of Civil and Environmental Engineering, Massachusetts Institute of Technology, Cambridge, MA 02139, USA.
*These authors contributed equally to this work.
†Corresponding author. Email: zhaox@mit.edu

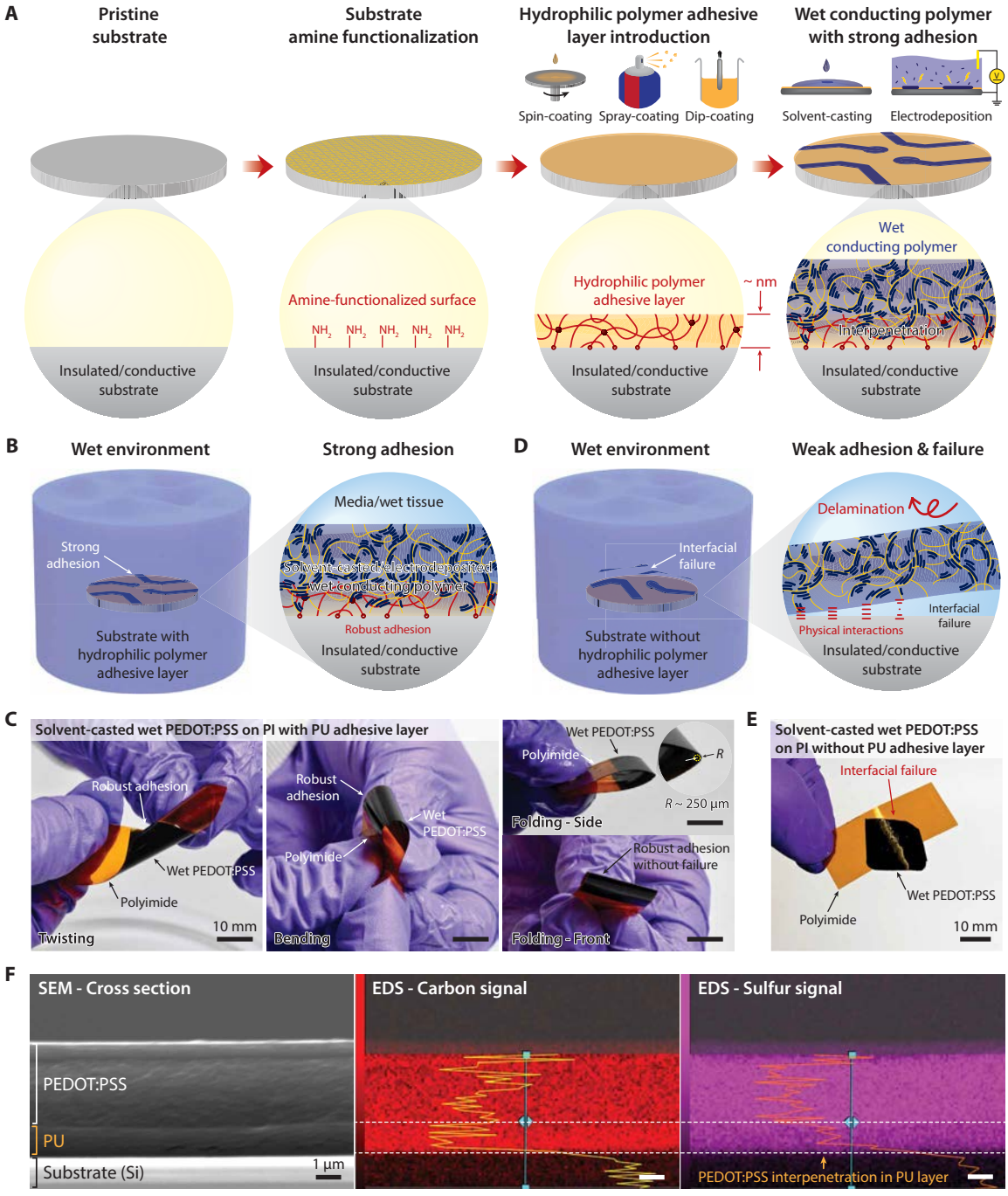

Fig. 1. Strong adhesion of wet conducting polymers on diverse substrates. (**A**) Strong adhesion of a wet conducting polymer on an amine-functionalized substrate with a hydrophilic polymer adhesive layer. (**B**) Strong adhesion of a conducting polymer on a substrate with an adhesive layer in wet environment. (**C**) Solvent-casted wet PEDOT:PSS (10 μm thickness) on a polyimide substrate with a PU adhesive layer (60 nm thickness) can withstand mechanical deformations including twisting, bending, and even folding (the radius of curvature ~ 250 μm) without interfacial failure. Photo credit: Hyunwoo Yuk, MIT. (**D**) Weak and unstable adhesion of a conducting polymer on a substrate without the adhesive layer in wet environment. (**E**) Solvent-casted wet PEDOT:PSS (10 μm thickness) on a polyimide substrate without the adhesive layer undergoes interfacial failure upon mechanical deformation of the substrate. Photo credit: Hyunwoo Yuk, MIT. (**F**) Distribution of carbon and sulfur atoms in a PU adhesive interface between an adhered PEDOT:PSS (5 μm thickness) and a PU-coated silicon substrate (1500 nm PU thickness).

precursors via various approaches such as solvent casting of aqueous conducting polymer solutions (e.g., PEDOT:PSS, PPy, and PAni) and electrodeposition of aqueous monomer solutions (e.g., EDOT:PSS). The hydrophilicity and subsequent swelling of the adhesive layer allow diffusion of the conducting polymer precursors throughout the adhesive layer (*29*), subsequently forming an interpenetrating polymer network between the infiltrated conducting polymer and the adhesive layer (*30*). The strong adhesion between the adhesive

layer and the substrate, and the interpenetration between the adhesive layer and the conducting polymer synergistically provide mechanically robust adhesion against interfacial failure in wet physiological environment (Fig. 1B). Furthermore, the conducting polymer interpenetrates throughout the adhesive layer and directly contacts the underlying substrate, providing electrical conductivity through the adhesive layer.

The proposed method can achieve strong adhesion of various wet conducting polymers on diverse substrates that are inaccessible to previous bonding methods. For example, a solvent-casted wet PEDOT:PSS on an insulating and flexible polyimide substrate with the PU adhesive layer exhibits robust adhesion without failure under twisting, bending, and even folding (with the radius of curvature ~ 250 μm) (Fig. 1C). In contrast, a wet PEDOT:PSS on substrates (e.g., glass and polyimide) without the PU adhesive layer exhibits interfacial failure upon swelling in phosphate-buffered saline (PBS; Fig. 1, D and E, and fig. S3B) due to weak and unstable adhesion formed by physical interactions of wet conducting polymers with the substrate surfaces (Fig. 1D) (*23*). To validate the formation of an interpenetrating layer between a conducting polymer and a hydrophilic PU adhesive layer, we investigate an elemental dispersion of carbon and sulfur atoms in a cross section of the PU adhesive layer of a cryo-fractured sample (solvent-casted PEDOT:PSS on Si wafer with the PU adhesive layer) by scanning electron microscopy–energy-dispersive x-ray spectroscopy (SEM-EDS). Because both PEDOT and PSS contain sulfur, while the hydrophilic PU is absent of sulfur (fig. S4), the sulfur signal can serve as an indicator for the interpenetration of the PEDOT:PSS into the PU adhesive layer. It is evident that the sulfur signal can be detected in the PU adhesive layer, indicating the interpenetration of the PEDOT:PSS throughout the PU adhesive layer (Fig. 1F). We further investigate the interpenetration between the PEDOT:PSS and the PU adhesive layer by comparing x-ray photoelectron spectroscopy (XPS) spectra of the surface of a wet PEDOT:PSS and the surfaces of 60-nm and 1500-nm PU adhesive layers with PEDOT:PSS interpenetrated from the other side (fig. S5; see the Supplementary Materials for preparation and testing of the samples). We find that the thin PU adhesive layer (60 nm) exhibits almost the same sulfur S(2p) spectral intensity as the PEDOT:PSS layer (fig. S5, D and E), whereas the thick PU adhesive layer (1500 nm) shows substantially lower sulfur S(2p) spectral intensity compared to the PEDOT:PSS layer (fig. S5F). These results indicate that the conducting polymer can interpenetrate throughout the thin adhesive layer (60 nm) but only partially through the thick adhesive layer (1500 nm).

Adhesion strength of wet conducting polymers on diverse substrates

To measure adhesion strength of wet conducting polymers on diverse substrates, we perform lap-shear tests to measure interfacial shear strength (ASTM D3163) between the adhered wet conducting polymer and the substrate (Fig. 2). Figure 2A shows a typical lap-shear test sample and a setup in which a wet conducting polymer is sandwiched between a hydrophilic microporous nylon filter (pore size, 1 μm) and a substrate with the PU adhesive layer. Note that we choose hydrophilic microporous nylon filters as the backing for the laboratory-shear tests due to two reasons: (i) The nylon filters' high mechanical stiffness (Young's modulus, >1 GPa) can prevent undesirable deformation of wet conducting polymers during lap-shear tests. (ii) Hydrophilicity and microporosity of the nylon filters allow infiltration of conducting polymers and subsequent reliable mechanical integration during lap-shear tests. Wet PEDOT:PSS on glass substrates with the PU adhesive layers exhibits a high shear strength (54 kPa), while wet PEDOT:PSS on pristine glass substrates without the PU adhesive layer shows a very low shear strength (0.08 kPa) and easily detaches from the substrate (Fig. 2, B and C).

We further investigate the effect of surface functionalization of substrates with primary amine groups on the adhesion performance. We compare shear strength and modes of failure in lap-shear tests for wet PEDOT:PSS on PU-coated glass substrates with and without primary amine functionalization. The wet PEDOT:PSS on the amine-functionalized glass substrate with the PU adhesive layer exhibits cohesive failure (i.e., failure occurs within wet PEDOT:PSS) (Fig. 2C), while the wet PEDOT:PSS on the pristine glass substrate with the PU adhesive layer demonstrates adhesive failure (i.e., failure occurs between the PU adhesive layer and the substrate) (Fig. 2B). Moreover, the amine-functionalized glass substrate with the PU adhesive layer provides a much higher shear strength than the pristine glass substrate with the PU adhesive layer (160 kPa versus 54 kPa) (Fig. 2D and fig. S6A). Hence, the amine functionalization is a critical step to achieve strong adhesion between the PU adhesive layer and the substrate due to enhanced adhesion of hydrophilic PU on amine-functionalized substrates (*30*). We also find that the PU adhesive layer can provide strong adhesion of wet PEDOT:PSS (shear strength over 120 kPa) consistently over a wide range of the PU layer's thickness (6 to 1500 nm) (fig. S7).

The proposed method is also applicable to various wet conducting polymers as well as a wide range of insulating and conductive substrates (Fig. 2, E and F). Solvent-casted wet PEDOT:PSS, PPy, and PAni on amine-functionalized glass substrates with the PU adhesive layers provide substantially higher shear strengths than the counterparts on pristine glass substrates without the PU adhesive layer (160 kPa versus 0.1 kPa for PEDOT:PSS; 39 kPa versus 0.4 kPa for PPy; 37 kPa versus 1.9 kPa for PAni) (Fig. 2E). Note that all conducting polymers undergo cohesive failure in the laboratory-shear tests, indicating that the adhesive interface with the PU adhesive layer is stronger than the bulk wet conducting polymer and that the measured adhesion strength is determined by the shear strength of the bulk wet conducting polymer. The proposed method also enables strong adhesion of wet PEDOT:PSS on diverse amine-functionalized insulating and conductive substrates including glass (shear strength, 160 kPa), polyimide (shear strength, 116 kPa), PDMS (shear strength, 111 kPa), ITO-glass (shear strength, 149 kPa), and gold (shear strength, 146 kPa) (Fig. 2F and figs. S6 and S8). We find that wet PEDOT:PSS on polyimide substrates with the PU adhesive layers exhibits negligible enhancement in the shear strength by amine functionalization (fig. S6C), which might result from good inherent adhesion of the hydrophilic PU on polyimide (fig. S9).

Electrical and mechanical properties of adhered wet conducting polymers

While the hydrophilic PU adhesive layers can provide strong adhesion between wet conducting polymers and substrates, they should not affect the electrical or mechanical properties of the conducting polymers in applications. To investigate this requirement, we systematically characterize the electrical and mechanical properties of PEDOT:PSS adhered by the PU adhesive layer as a representative conducting polymer (Fig. 3 and fig. S10). We measure the electrical conductivity of wet PEDOT:PSS without and with the PU adhesive

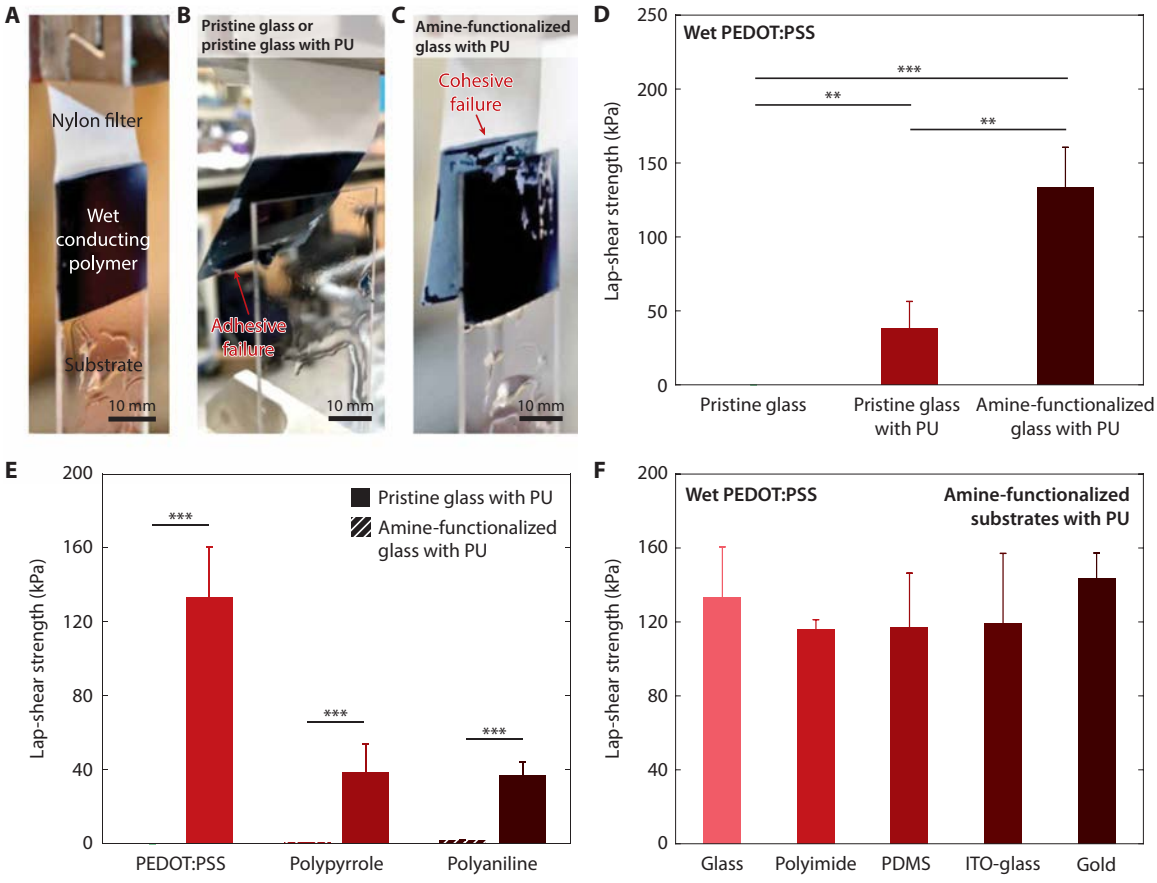

Fig. 2. Strong adhesion of wet conducting polymers on diverse substrates. (**A**) Image of a lap-shear test setup. Photo credit: Hyunwoo Yuk, MIT. (**B**) Image of adhesive failure during a lap-shear test of a wet PEDOT:PSS adhered on a pristine glass or a pristine glass with the PU adhesive layer. Photo credit: Hyunwoo Yuk, MIT. (**C**) Image of cohesive failure during a lap-shear test of a wet PEDOT:PSS adhered on an amine-functionalized glass with the PU adhesive layer. Photo credit: Hyunwoo Yuk, MIT. (**D**) Lap-shear strengths of wet PEDOT:PSS on a pristine glass substrate without the PU adhesive layer, a pristine glass substrate with the PU adhesive layer, and an amine-functionalized glass substrate with the PU adhesive layer. (**E**) Lap-shear strengths of various wet conducting polymers (PEDOT:PSS, PPy, and PAni) on pristine glass substrates without the PU adhesive layer and amine-functionalized glass substrates with the PU adhesive layer. (**F**) Lap-shear strengths of a wet PEDOT:PSS on various amine-functionalized insulating and conductive substrates with the PU adhesive layers. Conducting polymers with 50 μm thickness and PU adhesive layers with 60 nm thickness were used for all experiments. Values in (C) to (E) represent the mean, and the error bars represent 95% CI of the measured values ($n = 5$). P values are determined by Student's t test. $^{**}P \leq 0.01$; $^{***}P \leq 0.001$.

layer of varying thickness by a standard four-point probe method in wet physiological environment (hydrated in PBS) (Fig. 3A). The electrical conductivity of the wet PEDOT:PSS exhibits no statistically significant differences ($P > 0.5$) over a wide range of the PU adhesive layer thickness (6 to 1500 nm), indicating insignificant effect of the PU adhesive layer on the electrical properties of wet PEDOT:PSS (Fig. 3B). To probe the effect of the PU adhesive layer on electrical conductivity between wet PEDOT:PSS and underlying electrodes, we measure the sheet resistance of the wet PEDOT:PSS on the amine-functionalized ITO-glass electrodes without (R_i) and with (R_{ii}) the PU adhesive layer (Fig. 3C). Notably, the nanometer-thick PU adhesive layer (6 or 60 nm) gives negligible change in the measured sheet resistance (i.e., sheet resistance ratio, $R_i/R_{ii} \sim 1$), while the micrometer-thick PU adhesive layer (1500 nm) results in substantially increased interfacial resistance (i.e., $R_i/R_{ii} << 1$) (Fig. 3D). As identified in the XPS characterizations, PEDOT:PSS can interpenetrate throughout the thin PU adhesive layer (60 nm) but only partially through the thick PU adhesive layer (1500 nm) (fig. S5, D to F). Hence, the thick PU adhesive layer can substantially increase the interfacial resistance between the wet conducting polymer and the underlying electrode, whereas the sufficiently thin (i.e., nanometers thick) PU adhesive layer can provide low interfacial resistance.

To further investigate the effect of the PU adhesive layer's thickness on electrical property of the adhesive interface, we perform electrochemical impedance spectroscopy (EIS) analysis of wet PEDOT:PSS on amine-functionalized ITO-glass electrodes without and with the PU adhesive layer (60 or 1500 nm thickness) (Fig. 3E and fig. S11) (*31*). It can be seen that the PEDOT:PSS adhered on the ITO-glass electrode via the thin PU adhesive layer (60 nm) can provide favorable electrical property (i.e., lower impedance than the bare ITO-glass electrode in the low frequency region) due to enhanced capacitance of the electrode from the adhered wet PEDOT:PSS (fig. S11, A and B). In addition, the thick PU adhesive layer (1500 nm) exhibits much lower capacitance and higher impedance than the thin PU adhesive layer (60 nm) (fig. S11C). These results indicate

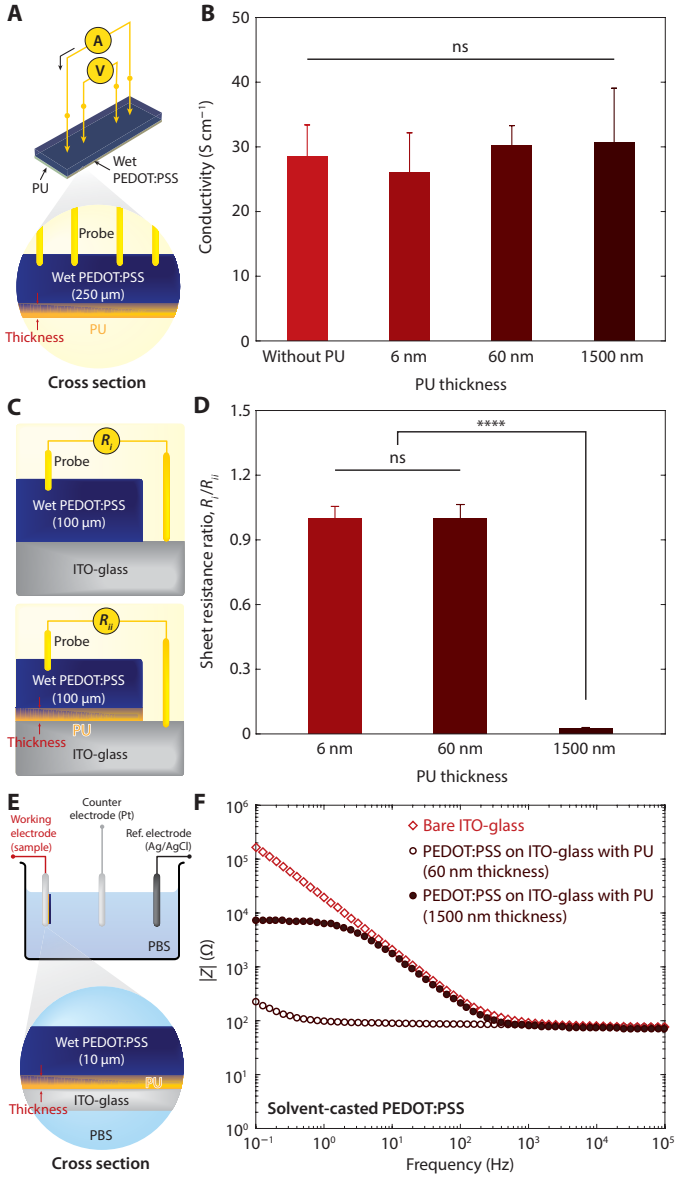

Fig. 3. Electrical properties of adhesive interface by varying PU adhesive layer thickness. (**A**) Schematic illustration of an electrical conductivity measurement setup for a wet PEDOT:PSS with the PU adhesive layer by the standard four-point probe method. (**B**) Conductivity of wet PEDOT:PSS with varying PU adhesive layer thickness. (**C**) Schematic illustration of a sheet resistance measurement setup for a wet PEDOT:PSS prepared on ITO-glass electrodes without and with the PU adhesion layer. (**D**) Sheet resistance ratio R_I/R_{II} between a wet PEDOT:PSS prepared on a ITO-glass electrode without the PU adhesion layer and a wet PEDOT:PSS prepared on a ITO-glass electrode with varying thickness of the PU adhesion layer. (**E**) Schematic illustration of an EIS setup for a wet PEDOT:PSS prepared on an ITO-glass electrode with the PU adhesion layer. (**F**) EIS curves for a bare ITO-glass electrode, a wet PEDOT:PSS (10 μm thickness) on an amine-functionalized ITO-glass electrode with the PU adhesive layer (60 nm thickness), and a wet PEDOT:PSS (10 μm thickness) on an amine-functionalized ITO-glass electrode with the PU adhesive layer (1500 nm thickness). Values in (B) and (D) represent the mean, and the error bars represent 95% CI of the measured values ($n = 5$). Statistical significance and P values are determined by one-way ANOVA and Tukey's multiple comparison test. ****$P \leq 0.0001$; ns, not significant.

that the nanometer-thick PU adhesive layer is essential to provide highly conductive interface between the adhered wet conducting polymers and the underlying electrodes.

To quantitatively evaluate the effect of the PU adhesive layer on the mechanical properties of wet PEDOT:PSS, we perform tensile tests of solvent-casted wet PEDOT:PSS in PBS without and with the PU adhesive layer of varying thickness (fig. S10A). The Young's moduli and the ultimate tensile strain of the wet PEDOT:PSS (100 μm thickness) with the PU adhesive layer of varying thickness (6 to 1500 nm) exhibit no statistically significant difference compared to the wet PEDOT:PSS without the PU adhesive layer ($P > 0.5$) (fig. S10, B and C). Hence, the PU adhesive layer can provide strong adhesion of wet PEDOT:PSS (fig. S12) without compromising the mechanical properties of wet PEDOT:PSS.

Mechanical and electrochemical stability of adhered wet conducting polymers

To ensure long-term functionality and reliability of bioelectronic devices in wet physiological environment, mechanical and electrochemical stability of conducting polymers on substrates is one of the most critical requirements. We evaluate the mechanical stability of adhered wet conducting polymers by characterizing interfacial failures and electrical properties of solvent-casted wet PEDOT:PSS on ITO-glass electrodes with the PU adhesive layers under prolonged ultrasonication in PBS (Fig. 4) (*23*). The solvent-casted PEDOT:PSS on the ITO-glass electrode without the PU adhesive layer undergoes complete interfacial delamination after ultrasonication for 1 min in PBS (Fig. 4A). In contrast, the solvent-casted PEDOT:PSS on the amine-functionalized ITO-glass electrode with the PU adhesive layer remains intact (Fig. 4B) and shows negligible deterioration in electrical property (Fig. 4C) after ultrasonication for 10 min in PBS, demonstrating superior mechanical stability of the adhesion. Furthermore, a solvent-casted wet PEDOT:PSS on an amine-functionalized PDMS substrate with the PU adhesive layer can withstand and remain intact without interfacial failure after 10,000 cycles of bending (radius of curvature ~ 2 mm) in PBS (movie S1).

We further investigate the electrochemical stability of adhered wet conducting polymers by evaluating the electrochemical properties of solvent-casted PEDOT:PSS on amine-functionalized Pt electrodes with the PU adhesive layers based on cyclic voltammetry (CV) tests in PBS (Fig. 4D) (*23*, *32*). The CV curves show a small change over 10,000 charging and discharging cycles with less than 6% decrease in charge storage capability (CSC) after 10,000 CV cycles, demonstrating superior electrochemical stability of the adhesion (Fig. 4, D and E). Moreover, the wet PEDOT:PSS on the Pt electrode with PU adhesive layer remains intact without any observable interfacial failure after 10,000 charging and discharging cycles (Fig. 4E).

The proposed method is also applicable to conducting polymers prepared by electrodeposition, which has been widely adopted to introduce conducting polymers on existing bioelectronic devices (*22*). To evaluate mechanical and electrochemical stability of electrodeposited conducting polymers adhered by the PU adhesive layer, we perform the same set of tests (i.e., ultrasonication, EIS, and CV) for electrodeposited PEDOT:PSS (fig. S13). Similar to solvent-casted PEDOT:PSS, the electrodeposited PEDOT:PSS on the ITO-glass electrodes with the PU adhesive layers exhibits superior mechanical stability against prolonged ultrasonication and electrochemical stability in wet physiological environment (fig. S13).

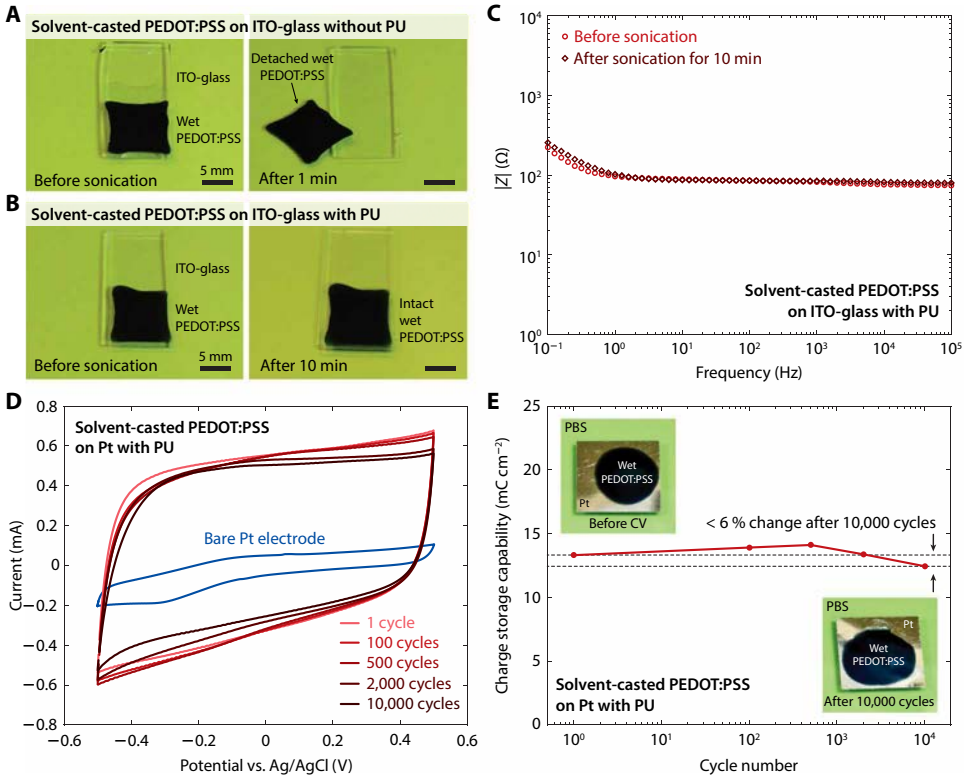

Fig. 4. Adhesion stability of solvent-casted wet conducting polymers. (**A**) Images of a solvent-casted wet PEDOT:PSS on a ITO-glass substrate without the PU adhesive layer before and after ultrasonication for 1 min. Photo credit: Hyunwoo Yuk, MIT. (**B**) Images of a solvent-casted wet PEDOT:PSS on an amine-functionalized ITO-glass substrate with the PU adhesive layer before and after ultrasonication for 10 min. Photo credit: Hyunwoo Yuk, MIT. (**C**) EIS curves for a solvent-casted wet PEDOT:PSS on amine-functionalized ITO-glass substrates with the PU adhesive layer before and after ultrasonication for 10 min. (**D**) Long-term CV curves for a solvent-casted wet PEDOT:PSS on an amine-functionalized Pt electrode with the PU adhesive layer in PBS. (**E**) Measured CSC versus CV cycle number for a solvent-casted wet PEDOT:PSS on an amine-functionalized Pt electrode with the PU adhesive layer in PBS. Photo credit: Hyunwoo Yuk, MIT. Conducting polymers with 10 μm thickness and PU adhesive layers with 60 nm thickness were used for all experiments.

Strong adhesion of wet conducting polymers on bioelectronic devices

While electrodeposited PEDOT:PSS has been intensively studied to improve electrical properties of various bioelectrodes (e.g., low impedance, high charge injection capacity, and low rigidity), poor long-term stability of the electrodeposited PEDOT:PSS on bioelectrodes in wet physiological environment has been one major hurdle that significantly limits their utility in practice (*17*, *23*, *24*, *27*). The new capability of forming strong, conductive, and mechanically and electrochemically stable adhesion between conducting polymers and diverse substrates allows us to readily electrodeposit conducting polymers on various existing bioelectronic devices, achieving high robustness in wet physiological conditions (Fig. 5).

Existing bioelectronic devices can be approximately classified into two categories based on configurations of their electrodes (*33*, *34*). In the first category, bioelectronic devices such as electrocorticography (ECoG) arrays (*35*), Michigan probes (*36*), and multielectrode arrays (MEA) consist of planar microelectrodes on the device substrates to provide bioelectronic sensing or stimulation (Fig. 5A). In the second category, bioelectronic devices such as Utah arrays (*37*), microwire electrode arrays (*38*), and fiber probes (*39*) consist of tip microelectrodes at end tips of the devices (Fig. 5B). To demonstrate flexibility and ready applicability of the proposed method to robustly integrate conducting polymers with various bioelectronic devices in wet physiological environment, we choose commercially available MEA with Au microelectrodes (Fig. 5C) and polytetrafluoroethylene (PTFE)–coated Pt microwire electrodes (Fig. 5F) as representative examples for bioelectronic devices with planar microelectrodes and tip microelectrodes, respectively.

Because of weak and unstable adhesion between electrodeposited PEDOT:PSS and Au electrodes, the electrodeposited PEDOT:PSS on the MEA (electrode diameter, 100 μm) without the PU adhesive layer undergoes deterioration in electrical property (Fig. 5C) and nearly disappears from the electrode surface after ultrasonication for 5 min in PBS (Fig. 5D). In contrast, the electrodeposited PEDOT:PSS on the MEA with the PU adhesive layer exhibits no observable change in electrical property (Fig. 5C) and remains intact after ultrasonication for 60 min in PBS (Fig. 5E), demonstrating strong adhesion and superior stability of the adhesion. Similarly, the electrodeposited PEDOT:PSS on the Pt microwire electrode (wire diameter, 100 μm) without the PU adhesive layer experiences deterioration in electrical property (Fig. 5F) and shows mechanical damage with the bare Pt electrode exposed after ultrasonication for 5 min in PBS (Fig. 5G and fig. S14). In contrast, the electrodeposited PEDOT:PSS on the Pt microwire electrode with the PU adhesive layer (only formed on Pt surface, not PTFE coating) exhibits negligible deterioration in electrical property (Fig. 5F) and mechanical

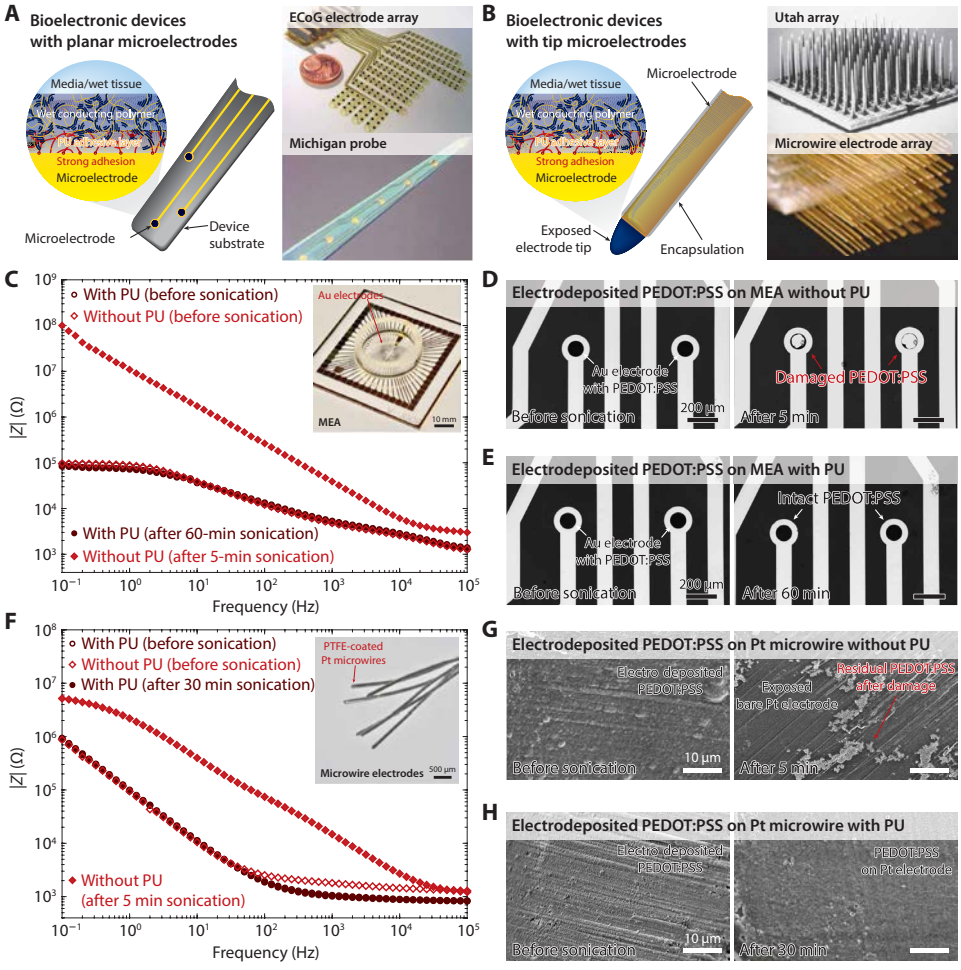

Fig. 5. Strong adhesion of wet conducting polymers on various bioelectronic devices. (**A**) Strong adhesion of wet conducting polymers on bioelectronic devices with planar microelectrodes. Images of the devices are reproduced with permission of IOP Publishing Ltd. from (*35*) (ECoG electrode array) and Wiley-VCH Verlag from (*36*) (Michigan probe). (**B**) Strong adhesion of wet conducting polymers on bioelectronic devices with tip-microelectrodes. Images of the devices are reproduced with permission of IEEE from (*37*) (Utah array) and National Academy of Sciences from (*38*) (microwire electrode array). (**C**) EIS curves for electrodeposited wet PEDOT:PSS on amine-functionalized Au electrodes of a commercially available microelectrode array (MEA) with and without the PU adhesive layer before and after ultrasonication in PBS. (**D**) Optical microscope images of an electrodeposited wet PEDOT:PSS on a MEA without the PU adhesive layer before and after ultrasonication for 5 min in PBS. (**E**) Optical microscope images of an electrodeposited wet PEDOT:PSS on an amine-functionalized MEA with the PU adhesive layer before and after ultrasonication for 60 min in PBS. (**F**) EIS curves for electrodeposited wet PEDOT:PSS on amine-functionalized commercially available PTFE-coated Pt microwire electrodes with and without the PU adhesive layer before and after ultrasonication in PBS. (**G**) SEM images of an electrodeposited PEDOT:PSS on a Pt microwire electrode without the PU adhesive layer before and after ultrasonication for 5 min in PBS. (**H**) SEM images of an electrodeposited PEDOT:PSS on an amine-functionalized Pt microwire electrode with the PU adhesive layer before and after ultrasonication for 30 min in PBS. Conducting polymers with 500 nm thickness and PU adhesive layers with 60 nm thickness were used for all experiments.

integrity after ultrasonication for 30 min in PBS (Fig. 5H and fig. S15).

CONCLUSION AND DISCUSSION

In this study, we present a general yet simple method to achieve strong adhesion of various wet conducting polymers on diverse substrates through intermediate hydrophilic polymer adhesive layers. While we choose the hydrophilic PU as the adhesive layer in this study, other hydrophilic polymers such as poly(vinyl alcohol) (PVA) may also be adopted as the adhesive layer (fig. S16). The proposed method can provide robust interfacial integration of various wet conducting polymers such as PEDOT:PSS, PPy, and PAni on a wide range of insulating and conductive substrates including glass, PDMS, polyimide, ITO, and gold as well as bioelectronic devices with representative form factors. The resultant conducting polymers adhered on substrates achieve superior adhesion performance (shear strength over 120 kPa) and remarkable mechanical and electrochemical stability without compromising electrical or mechanical properties of the conducting polymers. Our method is compatible with various fabrication approaches for conducting polymers including solvent casting and electrodeposition and allows the use of commercially accessible off-the-shelf materials (e.g., hydrophilic PU and conducting polymers), offering ready and broad applications in bioelectronic devices. The method also gives strong adhesion for very thin spin-coated conducting polymers (100 nm

thickness) in wet physiological environment (fig. S17). This study provides not only a simple yet effective method to solve the long-standing challenge of robust integration of conducting polymers in bioelectronic devices but also a general strategy to achieve strong adhesion between various hydrogels and substrates.

MATERIALS AND METHODS

Amine functionalization of diverse substrates

To functionalize glass, PDMS, and ITO-glass substrates with primary amine groups, substrates were first cleaned by washing with acetone and ethanol and deionized in sequence followed by drying under nitrogen flow. The cleaned substrates were then activated by an oxygen plasma cleaner (30 W at 20 mtorr pressure; Harrick Plasma) for 3 min (1 min for PDMS). After oxygen plasma treatment, the substrates were immersed in 50 ml of silane solution [10 μl of acetic acid, 1% (w/v) 3-aminopropyl trimethoxysilane in 100 ml of deionized water] for 1 hour at room temperature. After incubation in the silane solution, the substrates were thoroughly washed with deionized water and dried under nitrogen flow.

To functionalize Pt electrodes with primary amine groups, substrates were first cleaned by Piranha solution (3:1 mixture of concentrated sulfuric acid and 30% hydrogen peroxide solution). The cleaned substrates were then washed with deionized water and dried under nitrogen flow. The substrates were then immersed into 50 ml of silane solution [10 μl of acetic acid and 1% (w/v) 3-aminopropyl trimethoxysilane in 100 ml of deionized water] for 1 hour at room temperature. After incubation in the silane solution, the substrates were thoroughly washed with deionized water and dried under nitrogen flow.

To functionalize gold substrates or a MEA (with Au electrodes) with primary amine groups, substrates were first cleaned by washing with acetone and ethanol and deionized in sequence followed by drying under nitrogen flow. The cleaned substrates were then further cleaned by an oxygen plasma cleaner (30 W at 20 mtorr pressure; Harrick Plasma) for 3 min. After oxygen plasma treatment, the substrates were immersed into 50 ml of 1 mM aqueous cysteamine solution for 1 hour at room temperature. After incubation in the cysteamine solution, the substrates were thoroughly washed with deionized water and dried under nitrogen flow.

To functionalize polyimide substrates with primary amine groups, substrates were first cleaned by washing with acetone and ethanol and deionized in order followed by drying under nitrogen flow. The cleaned substrates were then immersed into 50 ml of 10% (w/v) aqueous hexamethylenediamine (HMDA) solution for 6 hours at room temperature. After incubation in the HMDA solution, the substrates were thoroughly washed with deionized water and dried under nitrogen flow.

Formation of strong adhesion of conducting polymers

A hydrophilic PU (HydroMed D3, AdvanSource Biomaterial) and a PVA (molecular weight = 124,000; Sigma-Aldrich) were used as PU adhesive layer and PVA adhesive layer, respectively. To prepare a hydrophilic PU solution, varying concentrations [1 to 5 weight % (wt %)] of PU were dissolved in mixture of ethanol and deionized water (95:5 = ethanol:water, v/v). To prepare a PVA solution, 1 wt % of PVA was dissolved in deionized water heated at 90°C. For planar substrates and devices in this study, the adhesive layer was introduced in a controlled manner by spin coating of the hydrophilic PU solution or the PVA solution at 2000 rpm for 30 s. For nonplanar substrates and devices in this study, the adhesive layer was introduced in controlled manner by dip-coating of the hydrophilic PU solution or the PVA solution with pulling rate of 1 cm min^{-1}. After spin coating or dip coating, the PU- or PVA-coated substrates were annealed at 80°C for 1 hour. In experiments, PU adhesive layer with 60 nm thickness was used unless otherwise mentioned. For strong adhesion of wet conducting polymers, conducting polymers were prepared by either solvent casting or electrodeposition on the PU- or PVA-coated substrates following the previously reported protocols (*10*, *23*, *40*, *41*).

For solvent-casted or spin-coated PEDOT:PSS, 15% (v/v) dimethyl sulfoxide was added into a commercially available aqueous PEDOT:PSS dispersion (Clevious PH1000, Heraeus Electric Materials) and vigorously stirred for 6 hours at room temperature. The mixed PEDOT:PSS dispersion was then filtered by PTFE filter (pore size, 5 μm) and solvent-casted or spin-coated on the PU- or PVA-coated substrates followed by air drying for 12 hours at room temperature and subsequent annealing for 30 min at 120°C. To obtain wet PEDOT:PSS adhered on the substrate, the samples were soaked in PBS for 1 hour before use.

For solvent-casted PPy, an aqueous pyrrole solution (0.3 M pyrrole and 0.1 M SDS in deionized water) and an aqueous oxidant solution (0.3 M ammonium persulfate in deionized water) were mixed in 1:1 by volume and vigorously stirred for 3 min at room temperature. The mixed solution was solvent-casted on the PU-coated substrates and incubated in ambient condition for 30 min. To obtain wet PPy adhered on the substrate, the samples were soaked in PBS for 1 hour before use.

For solvent-casted PAni, an aqueous aniline solution (1.42 M aniline and 1.42 M hydrochloric acid in deionized water) and an aqueous oxidant solution (1.42 M ammonium persulfate in deionized water) were mixed in 1:1 by volume and vigorously stirred for 1 min at 4°C. The mixed solution was solvent-casted on the PU-coated substrates and incubated in ambient condition for 30 min. To obtain wet PAni that adhered on the substrate, the samples were soaked in PBS for 1 hour before use.

For electrodeposited PEDOT:PSS, an EDOT:PSS precursor solution (0.02 M EDOT, 0.04 M PSS, and 0.1 M $LiClO_4$ in deionized water) was electropolymerized by an electrochemical potentiostat/galvanostat (PGSTAT30, Metrohm Autolab). A PU-coated electrode, a Pt sheet, and a Ag/AgCl wire were used as a working electrode, a counter electrode, and a reference electrode, respectively. The electropolymerization of EDOT was performed at 1.0 V versus Ag/AgCl (38 mC cm^{-2}) for ITO-glass substrates and at 1.0 V versus Ag/AgCl (43 mC cm^{-2}) for MEA with Au electrodes.

Measurement of adhesive layer thickness

The thickness of adhesive layers was measured by using an ellipsometer (Gaertner Scientific) with a wavelength at 633 nm. Changes in polarization were measured by the ellipsometer as a function of the sample thickness, which were then used to determine the thickness of the adhesive layers.

Elemental analysis and SEM imaging

Elemental distribution in adhesive interfaces was characterized by SEM-EDS measurement of a cross section of a dry PEDOT:PSS on a silicon substrate with the PU adhesive layer. The PEDOT:PSS on the amine-functionalized silicon substrate with the PU adhesive

layer was immersed in liquid nitrogen for 3 min and then cryo-fractured to obtain clean cross section. The cleaved sample was observed by using an SEM-EDS facility (6010LA, JEOL) and characterized to monitor the distribution of carbon and sulfur atoms. SEM images of bioelectronic devices with electrodeposited PEDOT:PSS were taken with the same SEM facility after Au sputtering (6 nm Au thickness).

Atomic force microscopy imaging

Atomic force microscopy (AFM) images and surface roughness data of diverse substrates were acquired by using an AFM facility (MFP-3D, Asylum Research). The substrates were directly attached onto the sample stage by double-sided carbon tape.

XPS characterizations

To prepare XPS samples, PEDOT:PSS was prepared by solvent-casting on a glass substrate, a glass substrate with the 60-nm PU adhesive layer, and a glass substrate with the 1500-nm PU adhesive layer. Before the sample preparation, the glass substrates were functionalized with perfluorosilane (1*H*, 1*H*, 2*H*, 2*H*-perfluorooctyltriethoxysilane) to aid the peel-off process of the samples from the glass substrates without residues of the PU adhesive layer or PEDOT:PSS. Subsequently, the PEDOT:PSS without and with the PU adhesive layer was peeled off from the glass substrate after swelling in PBS to expose the adhesion interface for XPS characterization. Surface chemical composition of the samples was characterized by using an XPS facility (VersaProbe II, Physical Electronics Inc.) under ultra-high vacuum of 5×10^{-10} mbar.

Mechanical characterizations

Before mechanical characterizations, all samples were immersed in PBS for 1 hour to hydrate the conducting polymers. Interfacial shear strength was measured by lap-shear tests (ASTM D3163) with an overlap area (length, 20 mm; width, 25 mm). The lap-shear test samples were prepared by solvent-casting of conducting polymers. A hydrophilic nylon filter (pore size, 1 μm; Tisch Scientific) was covered on top of a conducting polymer precursor solution on the substrate to provide a robustly integrated backing. The lap-shear tests were performed by using a mechanical testing machine (2-kN load cell, Zwick/Roell Z2.5) at the crosshead speed of 50 mm min^{-1}. The interfacial shear strength was determined by dividing the peak measured force by the overlap area. Tensile tests were performed in PBS bath with dog-bone shape samples by using a mechanical tester (UStretch, CellScale) to avoid dehydration of the wet conducting polymers during tests. Ultrasonication of samples was conducted by using a sonicator (VWR) with PBS bath at 25°C.

Electrical characterizations

Electrical conductivity was measured by using a standard four-point probe (SCS-4200, Keithley). Sheet resistance was measured by using a digital multimeter (Fluke) with an applied potential bias of 100 mV. All conducting polymer samples used for electrical conductivity and sheet resistance measurements were fully hydrated by immersing in PBS for 1 hour before the tests. EIS measurements were performed by using a potentiostat/galvanostat (1287A, Solartron Analytical) and a frequency response analyzer (1260A, Solartron Analytical) in an electrochemical cell installed with a wet PEDOT:PSS on an ITO-glass electrode (without or with the PU adhesive layer) as a working electrode, a Pt sheet as a counter electrode, a Ag/AgCl wire as a reference electrode, and PBS as an electrolyte. The frequency range between 0.1 and 100 kHz was scanned with an applied potential bias of 10 mV versus Ag/AgCl.

CV measurements were performed by using an electrochemical potentiostat/galvanostat (PGSTAT30, Metrohm Autolab) with a potential scan rate of 150 mV s^{-1} in an electrochemical cell installed with a wet PEDOT:PSS on a Pt electrode with the PU adhesive layer as a working electrode, a Pt sheet as a counter electrode, a Ag/AgCl wire as a reference electrode, and PBS as an electrolyte. The CSC of the sample was calculated from the measured CV data as

$$\mathrm{CSC} = \int_{E_2}^{E_1} \frac{i(E)}{2\nu A} dE$$

where ν is the scan rate, E_2 and E_1 are the potential window, i is the current at each potential, and A is the area of the wet PEDOT:PSS on Pt electrode, respectively.

Statistical analysis

MATLAB software was used to assess the statistical significance of all comparison studies in this work. Sample size of 5 was selected otherwise mentioned in all experiments. Data distribution was assumed to be normal for all parametric tests but not formally tested. In the statistical analysis for comparison between multiple samples, one-way ANOVA followed by Tukey's multiple comparison test were conducted with threshold of $^{*}P \leq 0.05$, $^{**}P \leq 0.01$, $^{***}P \leq 0.001$, and $^{****}P \leq 0.0001$. In the statistical analysis between two data groups, two-sample Student's t test was used, and significance threshold was placed at $^{*}P \leq 0.05$, $^{**}P \leq 0.01$, $^{***}P \leq 0.001$, and $^{****}P \leq 0.0001$. All error bars in the graphs represent the 95% confidence interval (CI) values.

SUPPLEMENTARY MATERIALS

Supplementary material for this article is available at http://advances.sciencemag.org/cgi/content/full/6/12/eaay5394/DC1

Fig. S1. Surface roughness of diverse substrates.
Fig. S2. Amine functionalization of diverse substrates.
Fig. S3. Strong adhesion of wet conducting polymer by PU adhesive layer.
Fig. S4. Chemical structures of hydrophilic PU, PEDOT, and PSS.
Fig. S5. XPS spectra of solvent-casted PEDOT:PSS with varying thickness of PU adhesive layer.
Fig. S6. Amine functionalization effect on lap-shear strength for diverse substrates.
Fig. S7. PU adhesive layer thickness effect on lap-shear strength for amine-functionalized glass substrate.
Fig. S8. Lap-shear test curves for diverse substrates.
Fig. S9. Adhesion of hydrophilic PU to polyimide.
Fig. S10. Mechanical properties of wet PEDOT:PSS with varying PU adhesive layer thickness.
Fig. S11. Nyquist plots for EIS measurements of adhesive interface by varying PU adhesive layer thickness.
Fig. S12. PU adhesive layer thickness effect on lap-shear strength for amine-functionalized ITO-glass substrates.
Fig. S13. Adhesion stability of electrodeposited wet conducting polymer.
Fig. S14. SEM images of electrodeposited PEDOT:PSS on Pt microwire electrode without PU adhesive layer.
Fig. S15. SEM images of electrodeposited PEDOT:PSS on amine-functionalized Pt microwire electrode with PU adhesive layer.
Fig. S16. Strong adhesion of wet conducting polymer by PVA adhesive layer.
Fig. S17. Adhesion of thin spin-coated conducting polymers in wet physiological environment.
Movie S1. Adhesion stability of wet PEDOT:PSS under cyclic bending deformations.

REFERENCES AND NOTES

1. S. Savagatrup, E. Chan, S. M. Renteria-Garcia, A. D. Printz, A. V. Zaretski, T. F. O'Connor, D. Rodriquez, E. Valle, D. J. Lipomi, Plasticization of PEDOT: PSS by common additives for mechanically robust organic solar cells and wearable sensors. *Adv. Funct. Mater.* **25**, 427–436 (2015).

2. S. Choi, H. Lee, R. Ghaffari, T. Hyeon, D.-H. Kim, Recent advances in flexible and stretchable bio-electronic devices integrated with nanomaterials. *Adv. Mater.* **28**, 4203–4218 (2016).
3. M. Kaltenbrunner, M. S. White, E. D. Głowacki, T. Sekitani, T. Someya, N. S. Sariciftci, S. Bauer, Ultrathin and lightweight organic solar cells with high flexibility. *Nat. Commun.* **3**, 770 (2012).
4. W. Honda, S. Harada, T. Arie, S. Akita, K. Takei, Wearable, human-interactive, health-monitoring, wireless devices fabricated by macroscale printing techniques. *Adv. Funct. Mater.* **24**, 3299–3304 (2014).
5. X. T. Cui, D. D. Zhou, Poly (3, 4-ethylenedioxythiophene) for chronic neural stimulation. *IEEE Trans. Neural Syst. Rehabil. Eng.* **15**, 502–508 (2007).
6. R. A. Green, R. T. Hassarati, L. Bouchinet, C. S. Lee, G. L. M. Cheong, J. F. Yu, C. W. Dodds, G. J. Suaning, L. A. Poole-Warren, N. H. Lovell, Substrate dependent stability of conducting polymer coatings on medical electrodes. *Biomaterials* **33**, 5875–5886 (2012).
7. H. S. Mandal, G. L. Knaack, H. Charkhkar, D. G. McHail, J. S. Kastee, T. C. Dumas, N. Peixoto, J. F. Rubinson, J. J. Pancrazio, Improving the performance of poly (3, 4-ethylenedioxythiophene) for brain–machine interface applications. *Acta Biomater.* **10**, 2446–2454 (2014).
8. D. Khodagholy, T. Doublet, P. Quilichini, M. Gurfinkel, P. Leleux, A. Ghestem, E. Ismailova, T. Hervé, S. Sanaur, C. Bernard, G. G. Malliaras, In vivo recordings of brain activity using organic transistors. *Nat. Commun.* **4**, 1575 (2013).
9. L. Groenendaal, F. Jonas, D. Freitag, H. Pielartzik, J. R. Reynolds, Poly (3, 4-ethylenedioxythiophene) and its derivatives: Past, present, and future. *Adv. Mater.* **12**, 481–494 (2000).
10. B. Lu, H. Yuk, S. Lin, N. Jian, K. Qu, J. Xu, X. Zhao, Pure PEDOT:PSS hydrogels. *Nat. Commun.* **10**, 1043 (2019).
11. J. Y. Kim, J. H. Jung, D. E. Lee, J. Joo, Enhancement of electrical conductivity of poly (3, 4-ethylenedioxythiophene)/poly (4-styrenesulfonate) by a change of solvents. *Synth. Met.* **126**, 311–316 (2002).
12. J. Rivnay, R. M. Owens, G. G. Malliaras, The rise of organic bioelectronics. *Chem. Mater.* **26**, 679–685 (2013).
13. M. Marzocchi, I. Gualandi, M. Calienni, I. Zironi, E. Scavetta, G. Castellani, B. Fraboni, Physical and electrochemical properties of PEDOT: PSS as a tool for controlling cell growth. *ACS Appl. Mater. Interfaces* **7**, 17993–18003 (2015).
14. Y. Wang, C. Zhu, R. Pfattner, H. Yan, L. Jin, S. Chen, F. Molina-Lopez, F. Lissel, J. Liu, N. I. Rabiah, Z. Chen, J. W. Chung, C. Linder, M. F. Toney, B. Murmann, Z. Bao, A highly stretchable, transparent, and conductive polymer. *Sci. Adv.* **3**, e1602076 (2017).
15. Y. Liu, A. F. McGuire, H.-Y. Lou, T. L. Li, J. B.-H. Tok, B. Cui, Z. Bao, Soft conductive micropillar electrode arrays for biologically relevant electrophysiological recording. *Proc. Natl. Acad. Sci. U.S.A.* **115**, 11718–11723 (2018).
16. V. R. Feig, H. Tran, M. Lee, Z. Bao, Mechanically tunable conductive interpenetrating network hydrogels that mimic the elastic moduli of biological tissue. *Nat. Commun.* **9**, 2740 (2018).
17. S. Venkatraman, J. Hendricks, Z. A. King, A. J. Sereno, S. Richardson-Burns, D. Martin, J. M. Carmena, In vitro and in vivo evaluation of PEDOT microelectrodes for neural stimulation and recording. *IEEE Trans. Neural Syst. Rehabil. Eng.* **19**, 307–316 (2011).
18. M. Berggren, A. Richter-Dahlfors, Organic bioelectronics. *Adv. Mater.* **19**, 3201–3213 (2007).
19. H. Yuk, T. Zhang, S. Lin, G. A. Parada, X. Zhao, Tough bonding of hydrogels to diverse non-porous surfaces. *Nat. Mater.* **15**, 190–196 (2016).
20. H. Yuk, T. Zhang, G. A. Parada, X. Liu, X. Zhao, Skin-inspired hydrogel–elastomer hybrids with robust interfaces and functional microstructures. *Nat. Commun.* **7**, 12028 (2016).
21. D. Wirthl, R. Pichler, M. Drack, G. Kettlguber, R. Moser, R. Gerstmayr, F. Hartmann, E. Bradt, R. Kaltseis, C. M. Siket, S. E. Schausberger, S. Hild, S. Bauer, M. Kaltenbrunner, Instant tough bonding of hydrogels for soft machines and electronics. *Sci. Adv.* **3**, e1700053 (2017).
22. H. Yuk, B. Lu, X. Zhao, Hydrogel bioelectronics. *Chem. Soc. Rev.* **48**, 1642–1667 (2019).
23. L. Ouyang, B. Wei, C.-c. Kuo, S. Pathak, B. Farrell, D. C. Martin, Enhanced PEDOT adhesion on solid substrates with electrografted P (EDOT-NH_2). *Sci. Adv.* **3**, e1600448 (2017).
24. C. Boehler, F. Oberueber, S. Schlabach, T. Stieglitz, M. Asplund, Long-term stable adhesion for conducting polymers in biomedical applications: IrOx and nanostructured platinum solve the chronic challenge. *ACS Appl. Mater. Interfaces* **9**, 189–197 (2016).
25. A. S. Pranti, A. Schander, A. Bödecker, W. Lang, Highly stable PEDOT:PSS coating on gold microelectrodes with improved charge injection capacity for chronic neural stimulation. *Proceedings* **1**, 492 (2017).
26. A. G. Sadekar, D. Mohite, S. Mulik, N. Chandrasekaran, C. Sotiriou-Leventis, N. Leventis, Robust PEDOT films by covalent bonding to substrates using in tandem sol–gel, surface initiated free-radical and redox polymerization. *J. Mater. Chem.* **22**, 100–108 (2012).
27. B. Wei, J. Liu, L. Ouyang, C.-C. Kuo, D. C. Martin, Significant enhancement of PEDOT thin film adhesion to inorganic solid substrates with EDOT-acid. *ACS Appl. Mater. Interfaces* **7**, 15388–15394 (2015).
28. H. P. Schreiber, R. Qin, A. Sengupta, The effectiveness of silane adhesion promoters in the performance of polyurethane adhesives. *J. Adhesion* **68**, 31–44 (1998).
29. S. Naficy, G. M. Spinks, G. G. Wallace, Thin, tough, pH-sensitive hydrogel films with rapid load recovery. *ACS Appl. Mater. Interfaces* **6**, 4109–4114 (2014).
30. M. Sasaki, B. C. Karikkineth, K. Nagamine, H. Kaji, K. Torimitsu, M. Nishizawa, Highly conductive stretchable and biocompatible electrode–hydrogel hybrids for advanced tissue engineering. *Adv. Healthc. Mater.* **3**, 1919–1927 (2014).
31. C. H. Hsu, F. Mansfeld, Technical note: Concerning the conversion of the constant phase element parameter Y0 into a capacitance. *Corrosion* **57**, 747–748 (2001).
32. M. Ganji, L. Hossain, A. Tanaka, M. Thunemann, E. Halgren, V. Gilja, A. Devor, S. A. Dayeh, Monolithic and scalable Au nanorod substrates improve PEDOT–Metal adhesion and stability in neural electrodes. *Adv. Healthc. Mater.* **7**, 1800923 (2018).
33. J. Rivnay, H. Wang, L. Fenno, K. Deisseroth, G. G. Malliaras, Next-generation probes, particles, and proteins for neural interfacing. *Sci. Adv.* **3**, e1601649 (2017).
34. R. Chen, A. Canales, P. Anikeeva, Neural recording and modulation technologies. *Nat. Rev. Mater.* **2**, 16093 (2017).
35. B. Rubehn, C. Bosman, R. Oostenveld, P. Fries, T. Stieglitz, A MEMS-based flexible multichannel ECoG-electrode array. *J. Neural Eng.* **6**, 036003 (2009).
36. M. R. Abidian, D. C. Martin, Multifunctional nanobiomaterials for neural interfaces. *Adv. Funct. Mater.* **19**, 573–585 (2009).
37. P. J. Rousche, R. A. Normann, Chronic intracortical microstimulation (ICMS) of cat sensory cortex using the Utah intracortical electrode array. *IEEE Trans. Rehabil. Eng.* **7**, 56–68 (1999).
38. M. A. L. Nicolelis, D. Dimitrov, J. M. Carmena, R. Crist, G. Lehew, J. D. Kralik, S. P. Wise, Chronic, multisite, multielectrode recordings in macaque monkeys. *Proc. Natl. Acad. Sci. U.S.A.* **100**, 11041–11046 (2003).
39. S. Park, Y. Guo, X. Jia, H. K. Choe, B. Grena, J. Kang, J. Park, C. Lu, A. Canales, R. Chen, Y. S. Yim, G. B. Choi, Y. Fink, P. Anikeeva, One-step optogenetics with multifunctional flexible polymer fibers. *Nat. Neurosci.* **20**, 612–619 (2017).
40. J. Bo, X. Luo, H. Huang, L. Li, W. Lai, X. Yu, Morphology-controlled fabrication of polypyrrole hydrogel for solid-state supercapacitor. *J. Power Sources* **407**, 105–111 (2018).
41. H. Guo, W. He, Y. Lu, X. Zhang, Self-crosslinked polyaniline hydrogel electrodes for electrochemical energy storage. *Carbon* **92**, 133–141 (2015).

Acknowledgments: We thank A. F. Schwartzman (MIT DMSE NanoMechanical Technology Laboratory) for help in AFM imaging. **Funding:** This work is supported by the National Science Foundation (CMMI-1661627). A.I. acknowledges the financial support from JSR Corporation. H.Y. acknowledges the financial support from Samsung Scholarship; B.L. acknowledges the financial support from the National Natural Science Foundation of China (51763010 and 51963011), Technological Expertise and Academic Leaders Training Program of Jiangxi Province (20194BCJ22013), and Research Project of State Key Laboratory of Mechanical System and Vibration (MSV202013). **Author contributions:** H.Y. conceived the idea. H.Y., A.I., and X.Z. designed the study. A.I. and H.Y. performed the experiments. A.I. and B.L. performed the electrochemical experiments. H.Y., A.I., B.L., and X.Z. analyzed and interpreted the results. H.Y. and X.Z. wrote the manuscript. X.Z. supervised the study. **Competing interests:** H.Y., A.I., and X.Z. are inventors of a U.S. patent application (U.S application no. 62/853,785) covering the strong adhesion of wet conducting polymers on diverse substrates and devices. **Data and materials availability:** All data needed to evaluate the conclusions in the paper are present in the paper and/or the Supplementary Materials. Additional data related to this paper may be requested from the authors.

Submitted 26 June 2019
Accepted 30 December 2019
Published 20 March 2020
10.1126/sciadv.aay5394

Citation: A. Inoue, H. Yuk, B. Lu, X. Zhao, Strong adhesion of wet conducting polymers on diverse substrates. *Sci. Adv.* **6**, eaay5394 (2020).

ScienceAdvances

Strong adhesion of wet conducting polymers on diverse substrates

Akihisa Inoue, Hyunwoo Yuk, Baoyang Lu and Xuanhe Zhao

Sci Adv **6** (12), eaay5394.
DOI: 10.1126/sciadv.aay5394

Science Advances
AAAS

advances.sciencemag.org/cgi/content/full/6/12/eaay5394/DC1

Supplementary Materials for

Strong adhesion of wet conducting polymers on diverse substrates

Akihisa Inoue, Hyunwoo Yuk, Baoyang Lu, Xuanhe Zhao*

*Corresponding author. Email: zhaox@mit.edu

Published 20 March 2020, *Sci. Adv.* **6**, eaay5394 (2020)
DOI: 10.1126/sciadv.aay5394

The PDF file includes:

Other Supplementary Material for this manuscript includes the following:

(available at advances.sciencemag.org/cgi/content/full/6/12/eaay5394/DC1)

Movie S1 (.mp4 format). Adhesion stability of wet PEDOT:PSS under cyclic bending deformations.

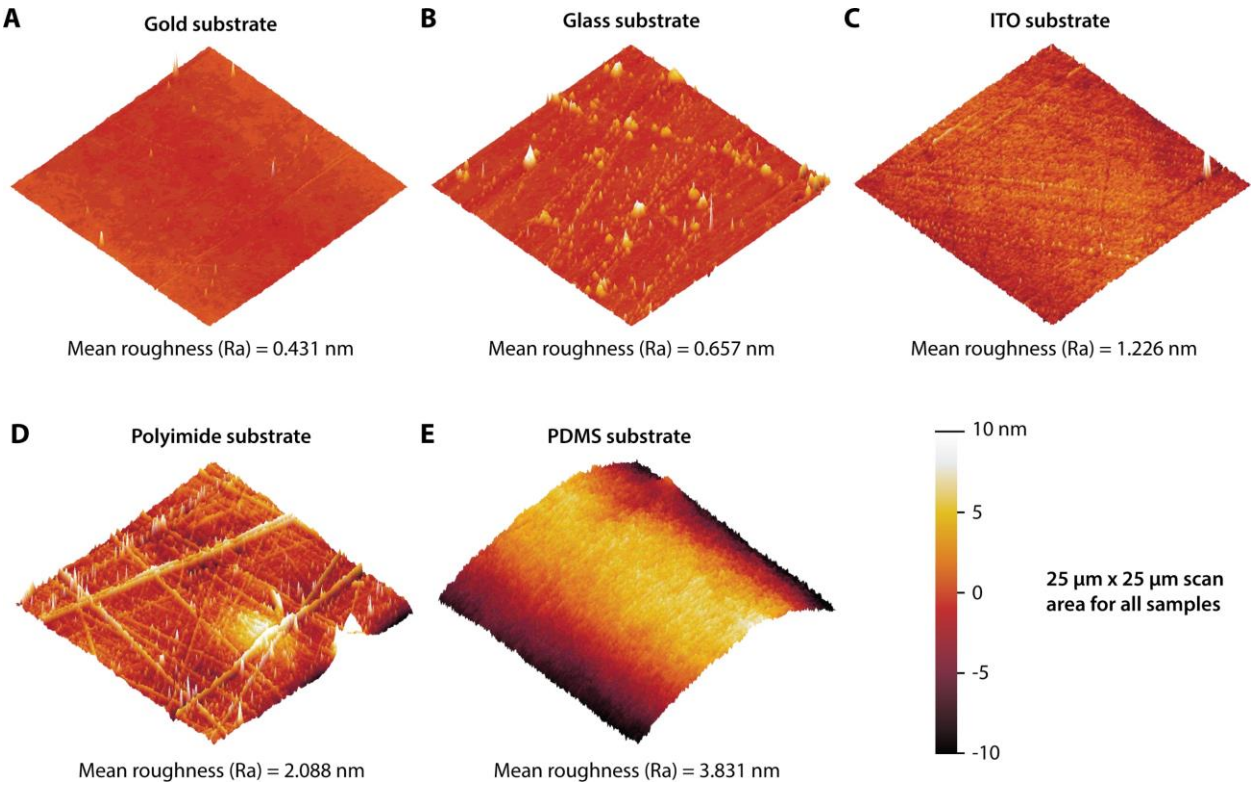

Fig. S1. Surface roughness of diverse substrates. (**A-E**) AFM characterizations of diverse substrates used for adhesion tests with small mean surface roughness (Ra) as 0.431 nm for gold (A), 0.657 nm for glass (B), 1.226 nm for ITO-glass (C), 2.088 nm for polyimide (D), and 3.831 nm for PDMS (E).

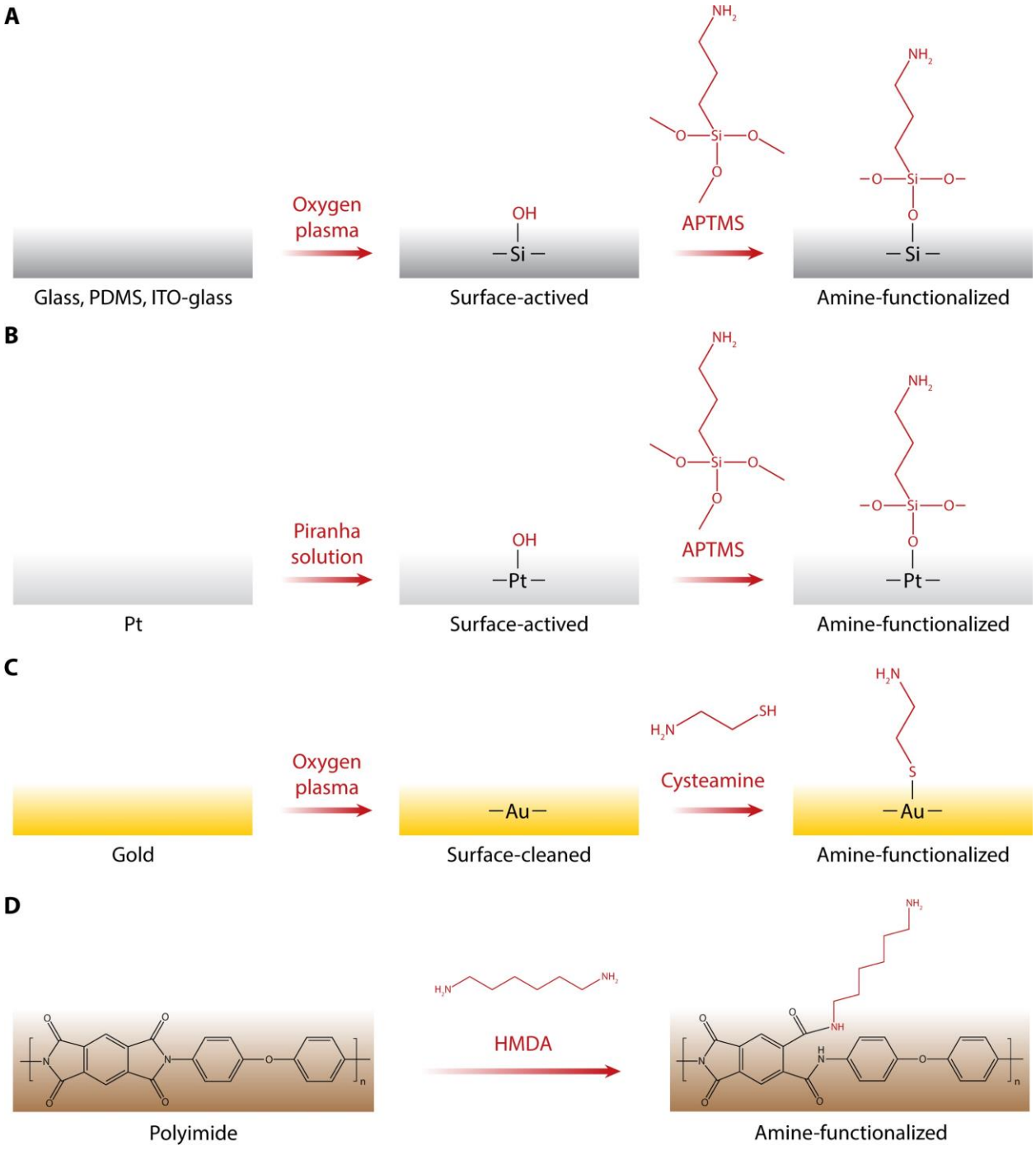

Fig. S2. Amine functionalization of diverse substrates. (**A-D**) Schematic illustrations for primary amine functionalization for glass (A), PDMS, ITO-glass, Pt (B), gold (C), and polyimide (D).

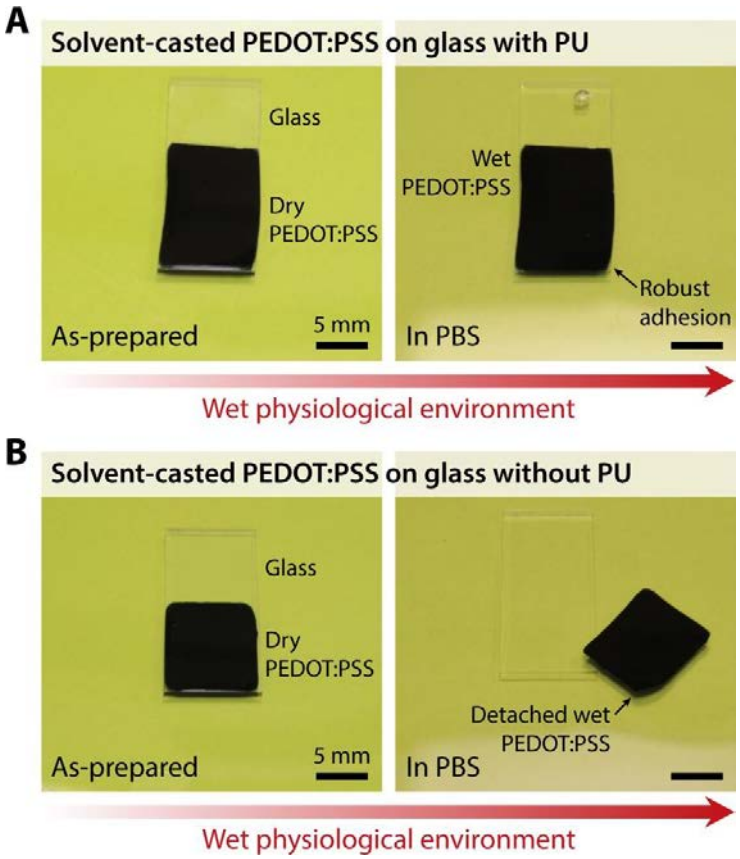

Fig. S3. Strong adhesion of wet conducting polymer by PU adhesive layer. (**A**,**B**) Images of a solvent-casted wet PEDOT:PSS on glass substrates with (A) and without (B) the PU adhesive layer in PBS. Conducting polymers with 50 μm thickness and PU adhesive layers with 60 nm thickness were used for all experiments. Photo Credit: Hyunwoo Yuk, MIT.

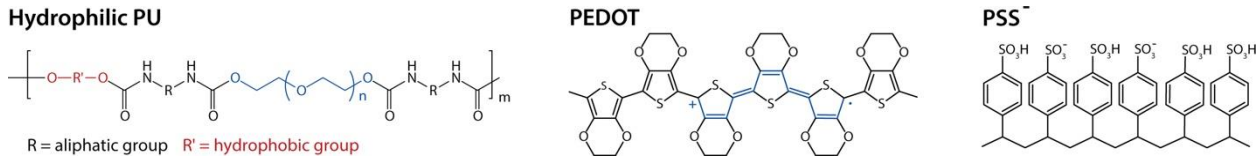

Fig. S4. Chemical structures of hydrophilic PU, PEDOT, and PSS.

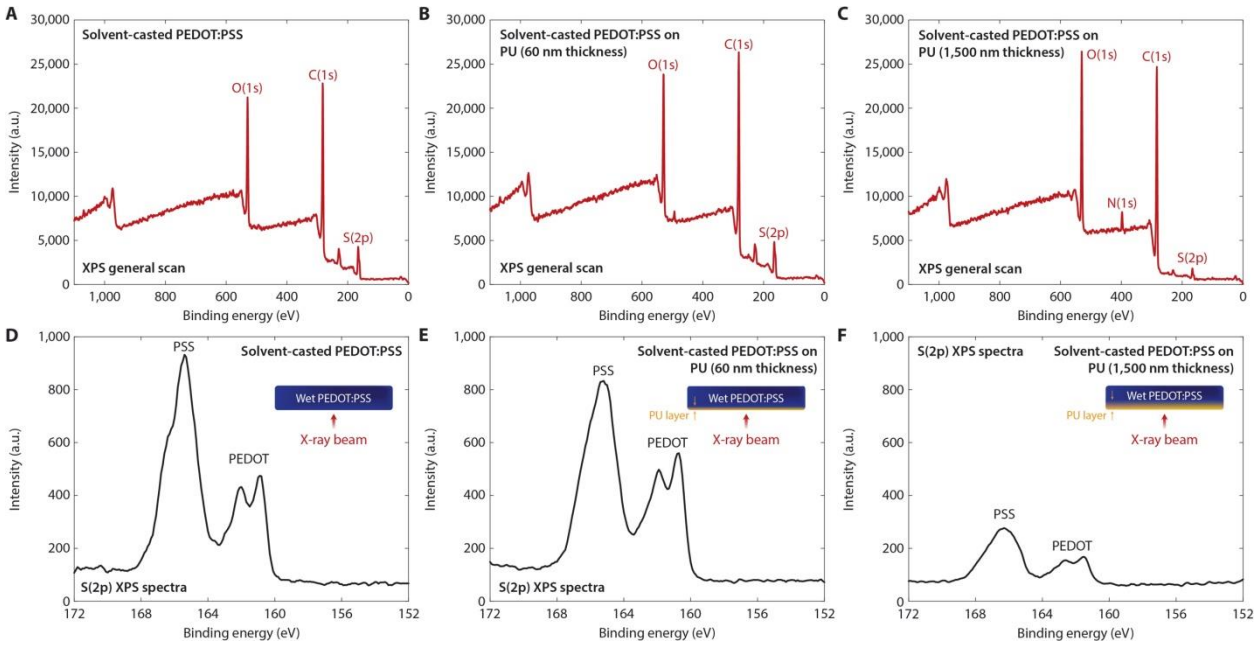

Fig. S5. XPS spectra of solvent-casted PEDOT:PSS with varying thickness of PU adhesive layer. (**A-C**) XPS general scan spectra for PEDOT:PSS without the PU adhesive layer (A), with the 60 nm PU adhesive layer (B), and the 1,500 nm PU adhesive layer (C). (**D-F**) XPS S(2p) (sulfur) spectra for PEDOT:PSS without the PU adhesive layer (D), with the 60 nm PU adhesive layer (E), and the 1,500 nm PU adhesive layer (F). Conducting polymers with 100 μm thickness were used for all experiments.

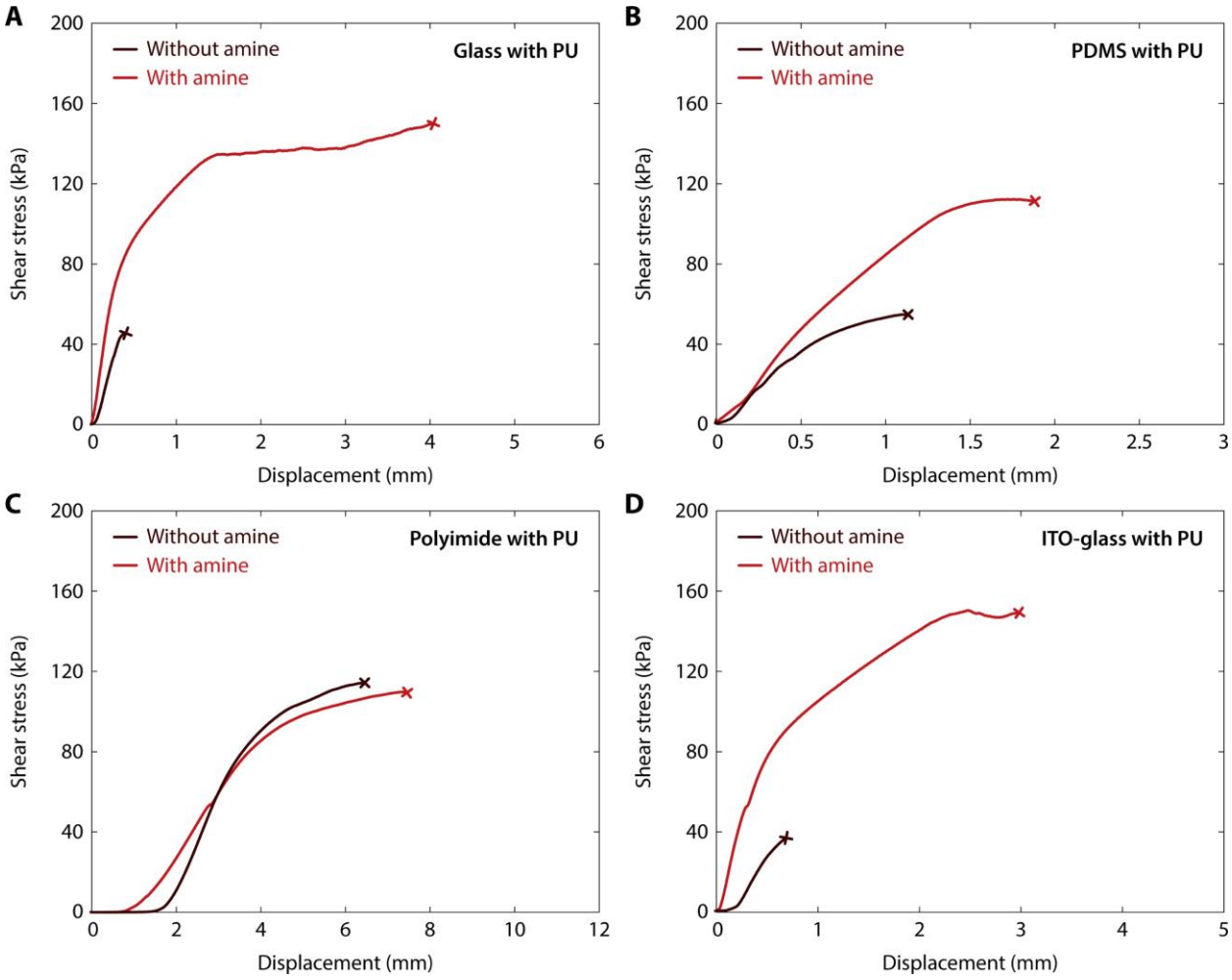

Fig. S6. Amine functionalization effect on lap-shear strength for diverse substrates. (**A-D**) Displacement vs. shear stress curves of lab-shear tests of wet PEDOT:PSS on PU-coated glass (A), PDMS (B), polyimide (C), and ITO-glass (D) substrates with and without primary amine functionalization. Conducting polymers with 10 μm thickness and PU adhesive layers with 60 nm thickness were used for all experiments.

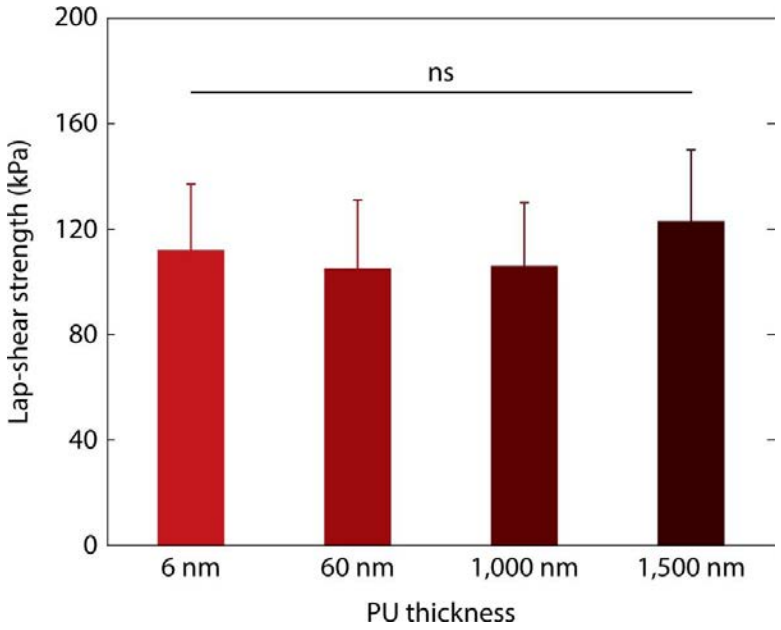

Fig. S7. PU adhesive layer thickness effect on lap-shear strength for amine-functionalized glass substrate. Conducting polymers with 10 μm thickness were used for all experiments. Values represent mean and the error bars represent 95% CI of the measured values (n = 5). Statistical significance and P values are determined by one-way ANOVA and Tukey's multiple comparison test. ns, not significant.

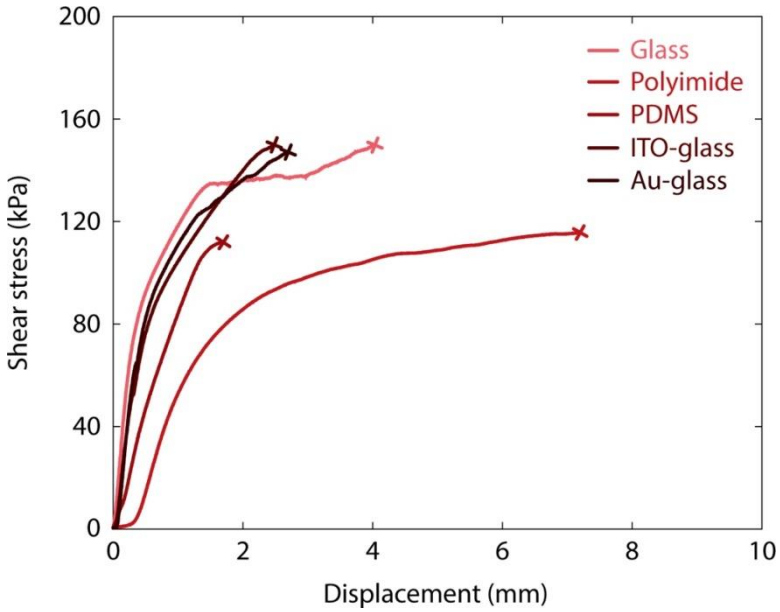

Fig. S8. Lap-shear test curves for diverse substrates. Conducting polymers with 10 μm thickness and PU adhesive layers with 60 nm thickness were used for all experiments.

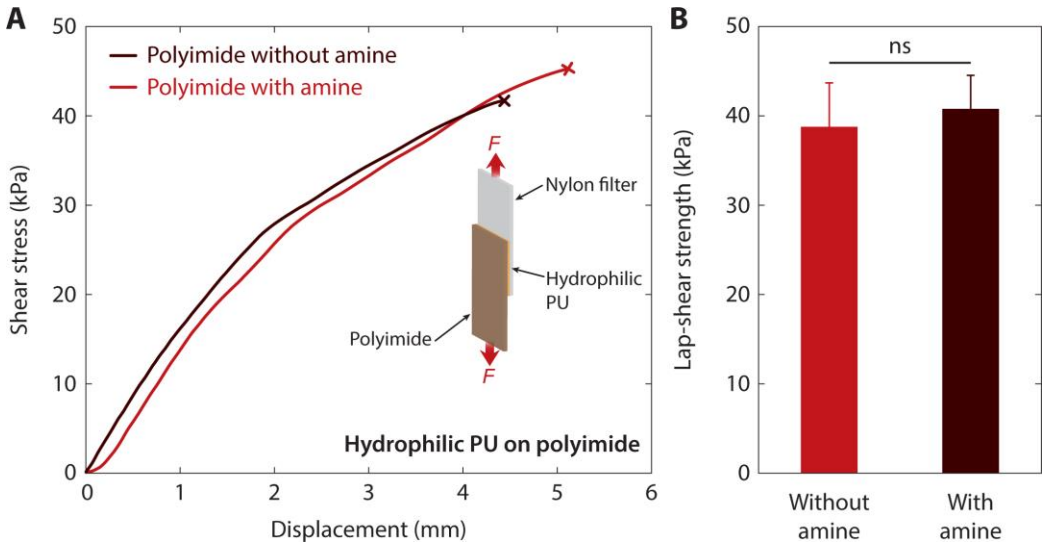

Fig. S9. Adhesion of hydrophilic PU to polyimide. (**A**) Displacement vs. shear stress curves from lab-shear tests of hydrophilic PU on polyimide substrates with and without primary amine functionalization. (**B**) Lap-shear strength of hydrophilic PU on polyimide substrates with and without primary amine functionalization. Hydrophilic PU layers with 10 μm thickness were used for all experiments. Values in **B** represent mean and the error bars represent 95% CI of the measured values ($n = 5$). *P* values are determined by Student's *t* test. ns, not significant.

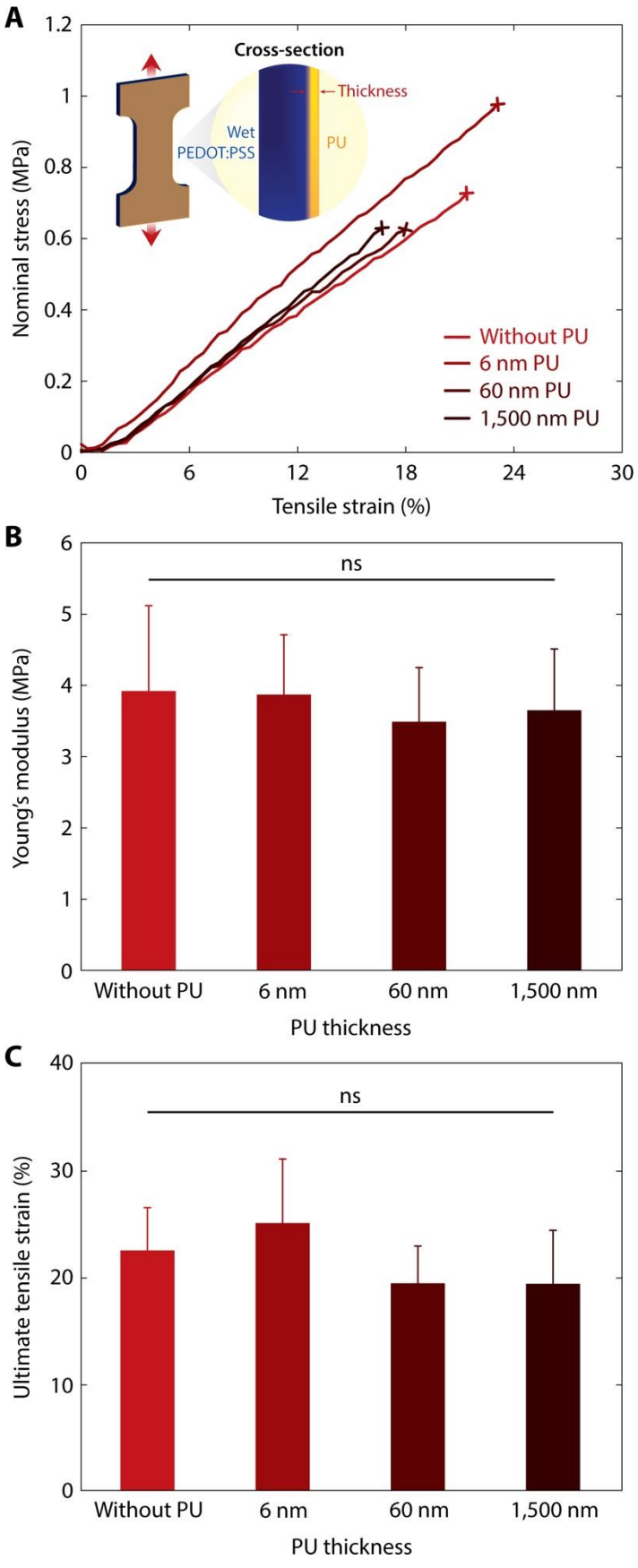
A
Cross-section
Thickness
Wet
PEDOT:PSS
PU
Nominal stress (MPa)
Tensile strain (%)
Without PU
6 nm PU
60 nm PU
1,500 nm PU
B
ns
Young's modulus (MPa)
Without PU
6 nm
60 nm
1,500 nm
PU thickness
C
ns
Ultimate tensile strain (%)
Without PU
6 nm
60 nm
1,500 nm
PU thickness

Fig. S10. Mechanical properties of wet PEDOT:PSS with varying PU adhesive layer thickness. (**A**) Nominal stress vs. tensile strain curves for wet PEDOT:PSS with the varying PU adhesive layer thickness. (**B**) Young's moduli of wet PEDOT:PSS with the varying PU adhesive layer thickness. (**C**) Ultimate tensile strain of wet PEDOT:PSS with the varying PU adhesive layer thickness. Values in **B**,**C** represent mean and the error bars represent 95% CI of the measured values (n = 5). Conducting polymers with 100 μm thickness were used for all experiments. Statistical significance and P values are determined by one-way ANOVA and Tukey's multiple comparison test. ns, not significant.

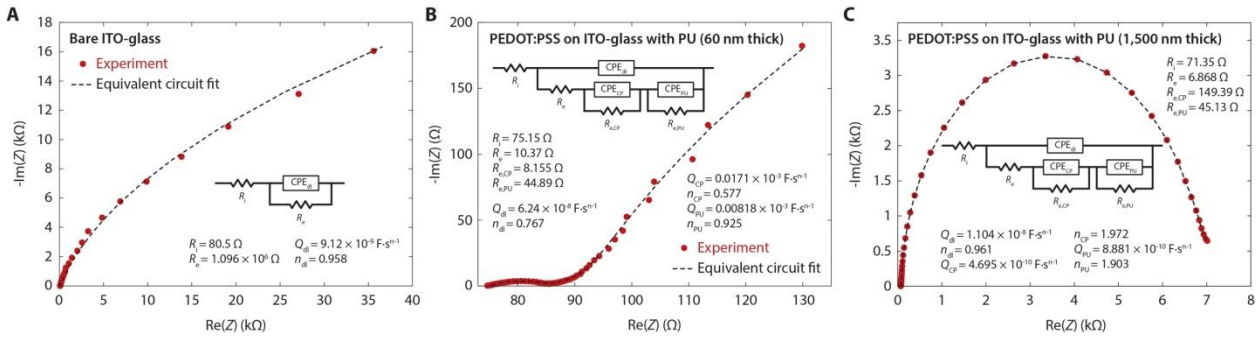

Fig. S11. Nyquist plots for EIS measurements of adhesive interface by varying PU adhesive layer thickness. (**A-C**) Nyquist plot obtained from the EIS measurement of a bare ITO-glass electrode (A), a wet PEDOT:PSS (10 μm thickness) on an amine-functionalized ITO-glass electrode with the PU adhesive layer (60 nm thickness) (B), and a wet PEDOT:PSS (10 μm thickness) on an amine-functionalized ITO-glass electrode with the PU adhesive layer (1,500 nm thickness) (C) overlaid with the plot predicted from the corresponding equivalent circuit models. In the equivalent circuit models, R_i represents ionic resistance for the electrolyte, R_e represents electronic resistance of the ITO-glass electrode, $R_{e,CP}$ represents electronic resistance of the wet conducting polymer, $R_{e,PU}$ represents electronic resistance of the PU adhesive layer, CPE_{dl} represents the double-layer capacitive phase element (CPE) for the ITO-glass electrode, CPE_{CP} represents CPE of the wet conducting polymer, and CPE_{PU} represents CPE of the PU adhesive layer. CPE is used to account inhomogeneous or imperfect capacitance, and are represented by the parameters Q and n where Q represents the peudocapacitance value and n represents the deviation from ideal capacitive behavior. The true capacitance C can be calculated from these parameters by using the relationship $C = Q\omega_{max}^{n-1}$, where ω_{max} is the frequency at which the imaginary component reaches a maximum.

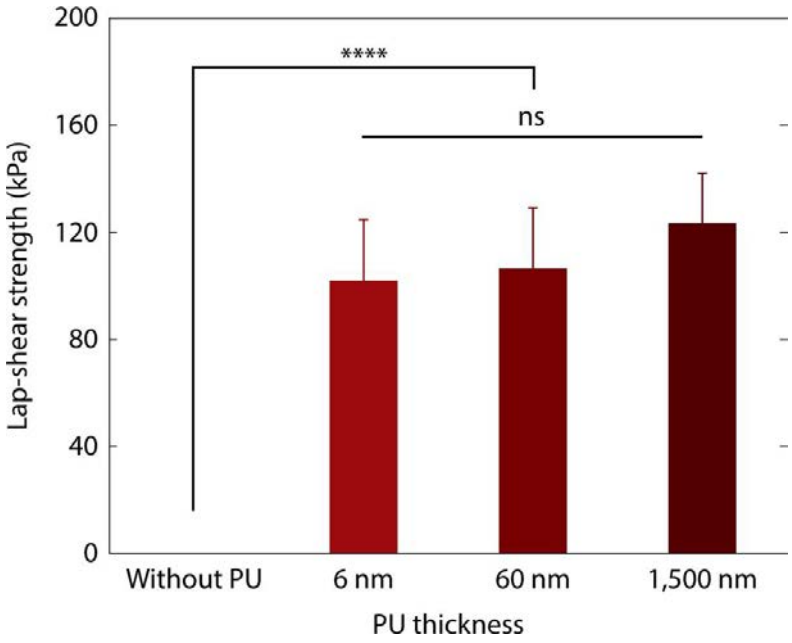

Fig. S12. PU adhesive layer thickness effect on lap-shear strength for amine-functionalized ITO-glass substrates. Conducting polymers with 50 μm thickness were used for all experiments. Values represent mean and the error bars represent 95% CI of the measured values ($n = 5$). Statistical significance and P values are determined by one-way ANOVA and Tukey's multiple comparison test. ****$P \leq 0.0001$; ns, not significant.

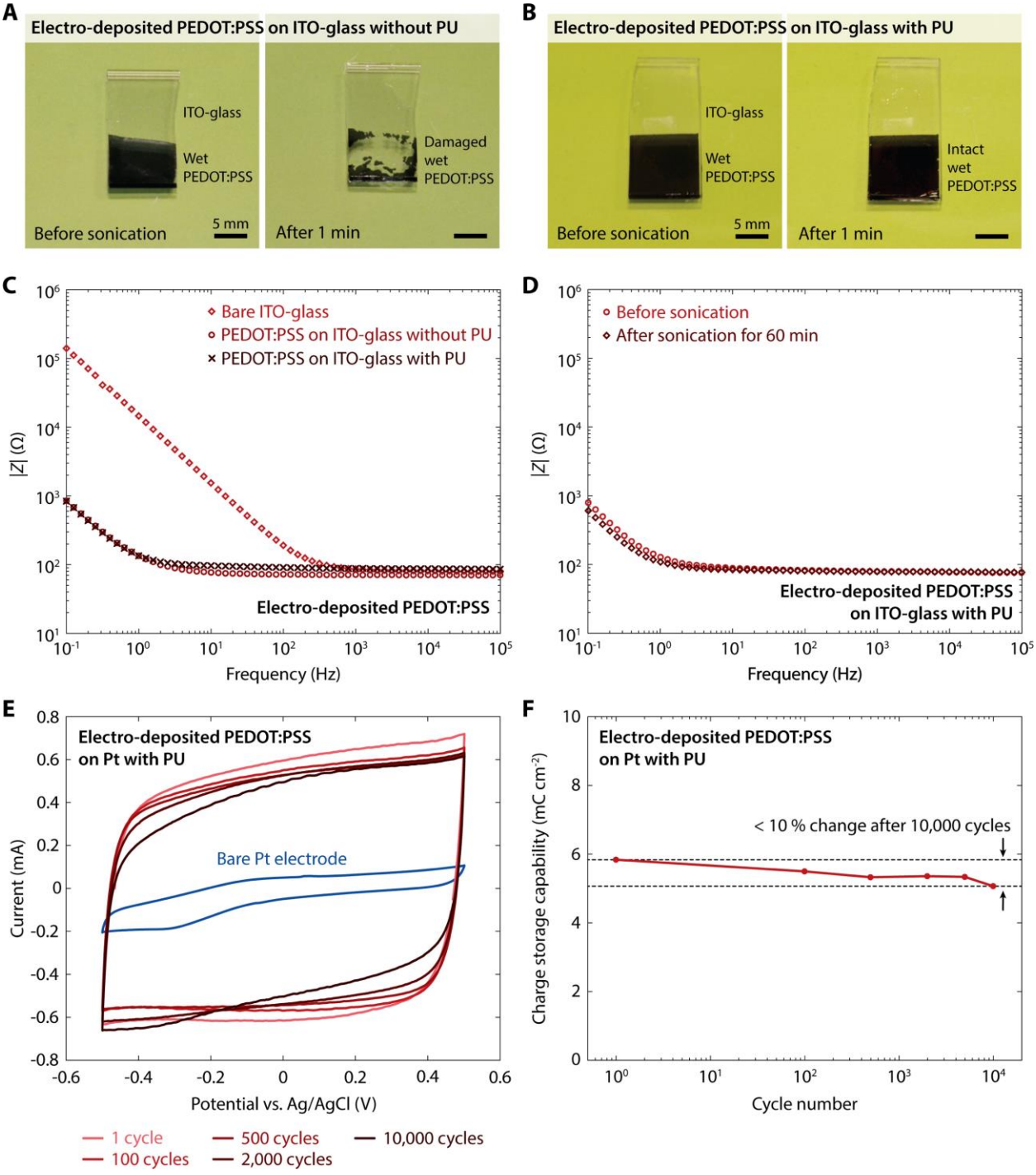
A
Electro-deposited PEDOT:PSS on ITO-glass without PU
ITO-glass
Wet PEDOT:PSS
Before sonication
5 mm
Damaged wet PEDOT:PSS
After 1 min
B
Electro-deposited PEDOT:PSS on ITO-glass with PU
ITO-glass
Wet PEDOT:PSS
Before sonication
5 mm
Intact wet PEDOT:PSS
After 1 min
C
Bare ITO-glass
PEDOT:PSS on ITO-glass without PU
PEDOT:PSS on ITO-glass with PU
Electro-deposited PEDOT:PSS
|Z| (Ω)
Frequency (Hz)
D
Before sonication
After sonication for 60 min
Electro-deposited PEDOT:PSS on ITO-glass with PU
|Z| (Ω)
Frequency (Hz)
E
Electro-deposited PEDOT:PSS on Pt with PU
Bare Pt electrode
Current (mA)
Potential vs. Ag/AgCl (V)
1 cycle
100 cycles
500 cycles
2,000 cycles
10,000 cycles
F
Electro-deposited PEDOT:PSS on Pt with PU
< 10 % change after 10,000 cycles
Charge storage capability (mC cm-2)
Cycle number

Fig. S13. Adhesion stability of electrodeposited wet conducting polymer. (**A**) Images of an electro-deposited wet PEDOT:PSS on a ITO-glass substrate without the PU adhesive layer before and after ultrasonication for 1 min. Photo Credit: Hyunwoo Yuk, MIT. (**B**) Images of an electro-deposited wet PEDOT:PSS on an amine-functionalized ITO-glass substrate with the PU adhesive layer before and after ultrasonication for 1 min. Photo Credit: Hyunwoo Yuk, MIT. (**C**) EIS curves for a ITO-glass electrode without the PU adhesive layer, an electro-deposited wet PEDOT:PSS on a ITO-glass electrode without the PU adhesive layer, and an electro-deposited wet PEDOT:PSS on an amine-functionalized ITO-glass electrode with the PU adhesive layer. (**D**) EIS curves for an electro-deposited wet PEDOT:PSS on an amine-functionalized ITO-glass electrode with the PU adhesive layer before and after ultrasonication for 60 min in PBS. (**E**) Long-term CV curves for an electro-deposited wet PEDOT:PSS on an amine-functionalized Pt electrode with the PU adhesive layer in PBS. (**F**) Measured CSC vs. CV cycle number for an electro-deposited wet PEDOT:PSS on an amine-functionalized Pt electrode with the PU adhesive layer in PBS. Conducting polymers with 500 nm thickness and PU adhesive layers with 60 nm thickness were used for all experiments.

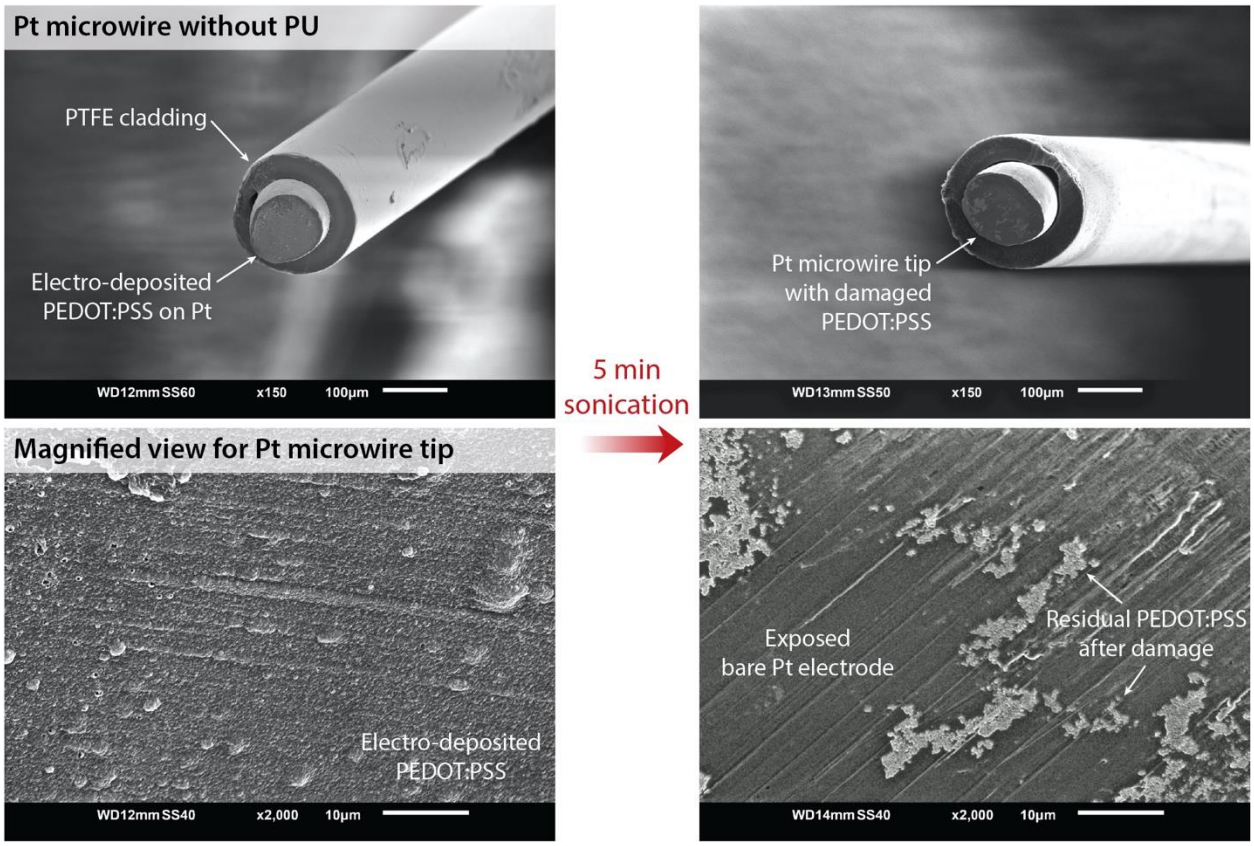

Fig. S14. SEM images of electrodeposited PEDOT:PSS on Pt microwire electrode without PU adhesive layer. Electro-deposited PEDOT:PSS on a Pt microwire electrode without the PU adhesive layer exhibits significant damage and delamination from the Pt electrode after ultrasonication for 5 min in PBS. Conducting polymers with 500 nm thickness and PU adhesive layers with 60 nm thickness were used for all experiments.

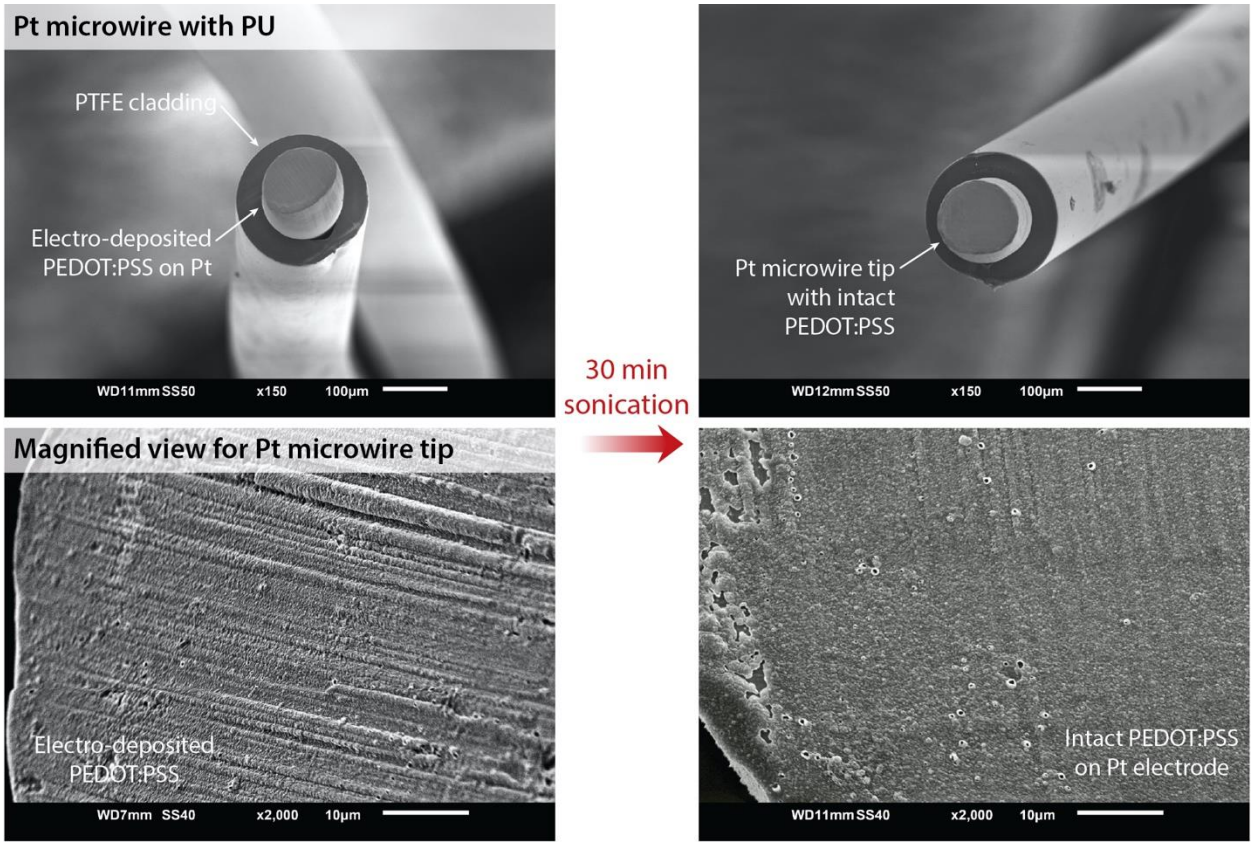

Fig. S15. SEM images of electrodeposited PEDOT:PSS on amine-functionalized Pt microwire electrode with PU adhesive layer. Electro-deposited PEDOT:PSS on an amine-functionalized Pt microwire electrode with the PU adhesive layer remains intact on the Pt electrode after ultrasonication for 30 min in PBS. Conducting polymers with 500 nm thickness and PU adhesive layers with 60 nm thickness were used for all experiments.

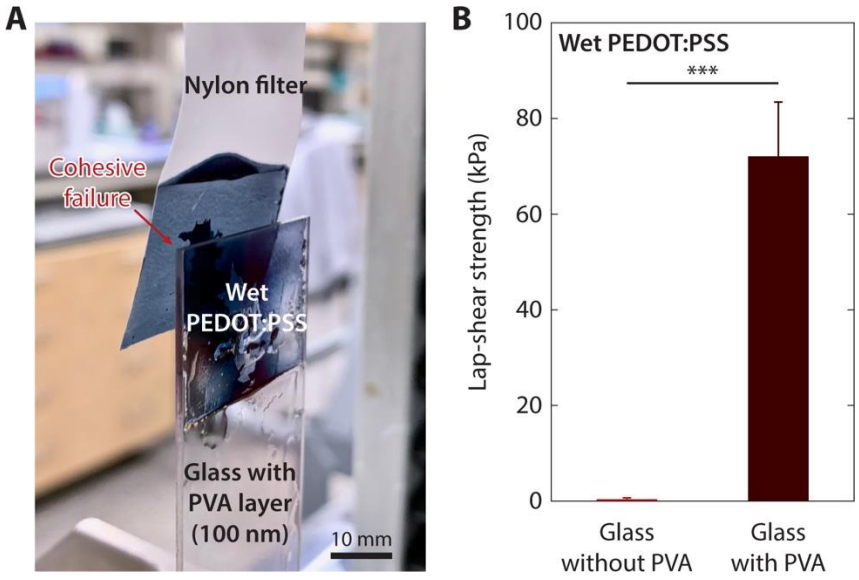

Fig. S16. Strong adhesion of wet conducting polymer by PVA adhesive layer. (**A**) Image of cohesive failure during lap-shear test for a wet PEDOT:PSS on a glass substrate with the PVA adhesive layer. Photo Credit: Hyunwoo Yuk, MIT. (**B**) Lap-shear strength of wet PEDOT:PSS on glass substrates with and without the PVA adhesive layer. Conducting polymers with 10 μm thickness and PVA adhesive layers with 100 nm thickness were used for all experiments. Values in **B** represent mean and the error bars represent 95% CI of the measured values ($n = 5$). P values are determined by Student's t test. ***$P \leq 0.001$.

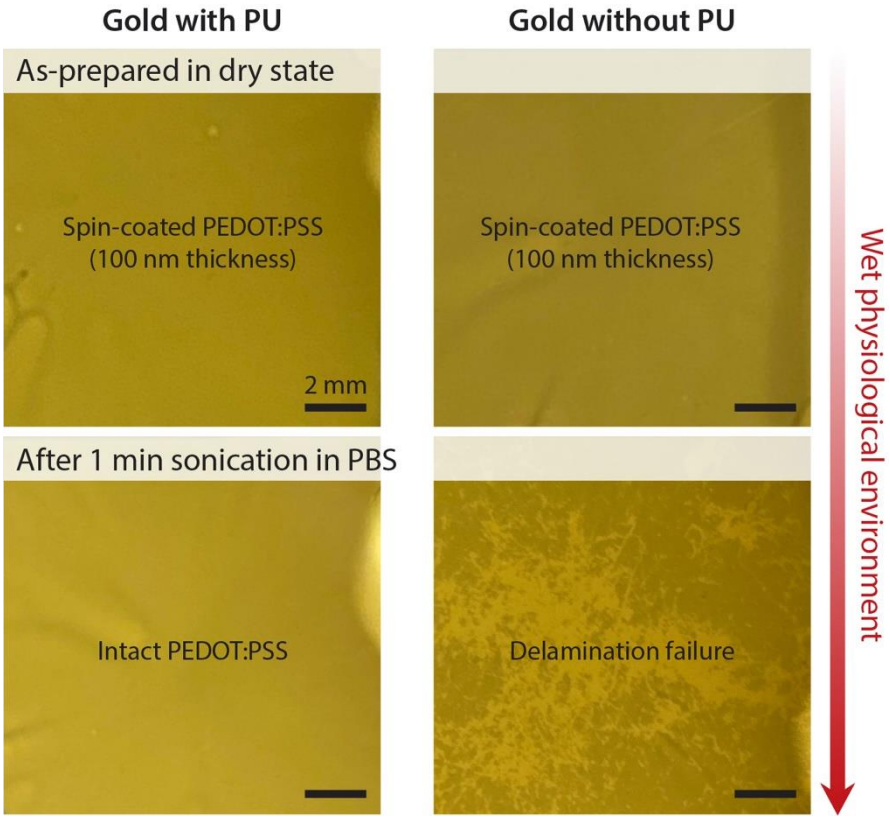

Fig. S17. Adhesion of thin spin-coated conducting polymers in wet physiological environment. Images of spin-coated PEDOT:PSS (~ 100 nm thickness) on gold substrates with and without the PU adhesive layer (60 nm thickness) after ultrasonication for 1 min in PBS. Photo Credit: Hyunwoo Yuk, MIT.

Legend for Supplementary Movie

Movie S1. Adhesion stability of wet PEDOT:PSS under cyclic bending deformations.